ASNC IMAGING GUIDELINES FOR NUCLEAR CARDIOLOGY PROCEDURES

PET myocardial perfusion and metabolism clinical imaging

Vasken Dilsizian, MD,[a] Stephen L. Bacharach, PhD,[b] Robert S. Beanlands, MD,[c] Steven R. Bergmann, MD, PhD,[d] Dominique Delbeke, MD,[e] Robert J. Gropler, MD,[f] Juhani Knuuti, MD, PhD,[g] Heinrich R. Schelbert, MD, PhD,[h] and Mark I. Travin, MD[i]

INTRODUCTION

Positron emission tomography (PET) utilizes radionuclide tracer techniques that produce images of in vivo radionuclide distribution using measurements made with an external detector system. Similar to computed tomography (CT), the images acquired with PET represent cross-sectional slices through the heart. However, with PET, the image intensity reflects organ function as opposed to anatomy. The functional information that is illustrated in PET images depends upon the radiopharmaceutical employed for that particular study. PET allows noninvasive evaluation of myocardial blood flow, function, and metabolism, using physiological substrates prepared with positron-emitting radionuclies, such as carbon, oxygen, nitrogen, and fluorine. These radionuclides have half-lives that are considerably shorter than those used in single photon emission CT (SPECT). Positron emitting radionuclides are produced using a cyclotron, such as fluoro-2-deoxyglucose (F-18 FDG) with a 110 minute half-life or a generator such as rubidium-82 (Rb-82) with a 75 second half-life.

PET radionuclides reach a more stable configuration by the emission of a positron. Positrons are positively charged particles with the same rest mass as electrons. When a positron collides with an electron, two 511 keV gamma rays are emitted. These emitted photons are nearly collinear, travelling in opposite directions, almost exactly 180° apart.[1]

The PET detectors are configured to register only photon pairs that strike opposing detectors at approximately the same time, termed coincidence detection. Over the course of a typical scan, millions of coincidence events are recorded and projections of the activity distribution are measured at all angles around the patient. These projections are subsequently used to reconstruct an image of the in vivo radionuclide distribution using the same algorithms as those used in x-ray CT. The resulting PET images have improved spatial and temporal resolution when compared to SPECT.

Recent advances in the instrumentation of multichannel spiral CT allow detailed visualization of the coronary arteries, noninvasively, as an adjunct to PET imaging. Whereas multichannel CT angiography provides information on the presence and extent of anatomical luminal narrowing of epicardial coronary arteries, stress myocardial perfusion PET provides information on the downstream functional consequences of such anatomic lesions. Thus, with hybrid PET/CT systems, such complementary information of anatomy and physiology can be obtained during the same imaging session. The ability to determine coronary artery disease, myocardial perfusion, viability, and ventricular function from a hybrid PET/CT system has the potential to be an important tool in the clinical practice of cardiology.

The current document is an update of an earlier version of PET guidelines that was developed by the American Society of Nuclear Cardiology.[2] The publication is designed to provide imaging guidelines for physicians and technologists who are qualified to practice nuclear cardiology. While the information supplied in this document has been carefully reviewed by experts in the field, the document should not be considered

This statement has been endorsed by the SNM-Advancing Molecular Imaging and Therapy.

From the University of Maryland Medical Center,[a] Baltimore, MD; UCSF,[b] San Francisco, CA; University of Ottawa Heart Institute,[c] Ottawa, Ontario, Canada; Beth Israel Medical Center,[d] New York, NY; Vanderbilt University Medical Center,[e] Nashville, TN; Washington University,[f] St. Louis, MO; Turku University Hospital,[g] Turku, Finland; UCLA School of Medicine,[h] Los Angeles, CA; Montefiore Medical Center,[i] Pleasantville, NY.

Unless reaffirmed, retired or amended by express action of the Board of Directors of the American Society of Nuclear Cardiology, this Imaging Guideline shall expire as of May 2014.

Reprint requests: Vasken Dilsizian, MD, University of Maryland Medical Center, Baltimore, MD.

1071-3581/$34.00

doi:10.1007/s12350-009-9094-9

medical advice or a professional service. We are cognizant that PET and PET/CT technology is evolving rapidly and that these recommendations may need further revision in the near future. Hence, the imaging guidelines described in this publication should not be used in clinical studies until they have been reviewed and approved by qualified physicians and technologists from their own particular institutions.

PET AND PET/CT INSTRUMENTATION

PET Imaging Systems (2D and 3D)

The majority of dedicated PET cameras consist of rings of small detectors that are typically a few millimeters on a side, and tens of millimeters deep. Coincidences between detectors in a single ring produce one tomographic slice of data. Usually one or more adjacent rings may also contribute to counts in that slice. In a 2-dimensional (2D) or ''septa-in'' PET scanner, there is a septum (e.g., lead or tungsten) between adjacent rings. This septum partially shields coincidences from occurring between detectors in one ring and detectors in a non-adjacent or more distant ring. By minimizing coincidences between a ring and its more distant neighboring rings, the septa greatly reduce scattered events.

A scanner with no septa in place is referred to as a three-dimensional (3D) or ''septa-out'' scanner. This permits coincidences between all possible pairs of detectors, greatly increasing sensitivity but also greatly increasing scatter. The increased sensitivity is the greatest for the central slice and falls rapidly, and usually linearly, for slices more distant from the central slice. The slices near the edge have the sensitivity of about the same as in a 2D scanner but with greater scatter. Scatter is measured with standards given by the National Electrical Manufacturers Association (NEMA)[3-5] and is typically in the order of 10-15% for 2D scanners and 30-40% or more for 3D scanners. In chest slices encompassing the heart, as opposed to the relatively small NEMA phantom, there is an even larger increase in scattered counts for 3D imaging. For cardiac applications, scatter tends to increase the counts in cold areas surrounded by higher-activity regions (e.g., a defect surrounded by normal uptake).

Some manufacturers have scanners that have retractable septa, permitting the user to choose between 2D and 3D operation. Many PET/CT manufacturers have opted for scanners that operate only in 3D mode, since these are preferred for oncology studies. Situations in which 3D mode may be advantageous include those in which:

1. Whole-body patient throughput is important (e.g., a busy oncology practice).
2. Radiation exposure is critical, so that reductions in injected activity are desired.
3. Special (i.e., usually research) radiopharmaceuticals are being used, which can only be produced in low radioactivity quantities.

As noted above, although 3D acquisition is in principle many times more sensitive than 2D, random events (termed randoms), dead time, and scatter can greatly reduce the effective sensitivity of images acquired in 3D, especially at high doses. Thus, in order to prevent poor quality images, lower doses are administered. When using 3D imaging with a bismuth germanate (BGO) crystal camera, for example, 3D imaging had often been used when the dose had to be minimized (e.g., in normal volunteers, in children, or when multiple studies are planned) or when scatter was minimal (e.g., brain imaging). The advent of lutetium oxyothosilicate (LSO)- and gadolinium oxyorthosilicate (GSO)-based PET scanners, and even BGO scanners with new-generation optimized photo multiplier/crystal coupling schemes and high-speed electronics, has made 3D imaging more practical. Improvements in software, coupled with improvements in electronics and crystal technology can, in part, compensate for the increase in randoms, dead time, and scattered events.[6] The use of 3D cardiac imaging with new-generation machines continues to be evaluated. The degree to which any of these improvements is achieved in practice for cardiac imaging may vary between manufacturers.

PET Imaging-Crystal Types

Four different crystal types are commonly employed—BGO, GSO, LSO, and lutetium yttrium orthosilicate (LYSO)—although other crystal types have also been used. Each of them can be used successfully for cardiac imaging. BGO has the highest stopping power, but relatively poor energy resolution (i.e., limiting energy-based scatter reduction) and timing resolution (i.e., limiting its ability to reduce randoms). GSO, LSO, and LYSO have better timing resolution and, in theory, better energy resolution. For 2D imaging, GSO, LSO, and LYSO may not offer significant advantage over BGO, given the inherently high sensitivity of BGO. The main advantage of the newer crystals is their much reduced dead time, which enables them to acquire data at the much higher count rates associated with operating in 3D mode, and to better minimize the effects of randoms. One minor disadvantage of LSO and LYSO is their intrinsic radioactivity, which contributes to a small increase to the random event rate.

The better energy resolution of GSO, LSO, or LYSO, and consequent reduction of scatter in 3D mode, would make these detector types advantageous. At present, the theoretical energy resolution for these detectors does not seem to have been fully realized in practice, leaving all three crystal types with similar energy-based scatter rejection (i.e., GSO, LSO, and LYSO giving only slight potential improvement over BGO) and making 2D imaging still the method of choice if scatter rejection is critical. Modern image reconstruction algorithms incorporate improved models for scatter correction, and as a result, the impact of scatter for state-of-the-art scanners operating in 3D mode is usually acceptable for clinical imaging. The suitability of 3D mode for cardiac PET imaging should be evaluated by the user.

PET TOF Imaging

Machines that incorporate time-of-flight (TOF) information in the acquisition process have recently been commercially introduced. TOF refers to the time difference between the two 511 keV annihilation photons reaching their respective detectors, 180° apart. For example, if the positron annihilation occurred at the center of the machine, the two photons would reach their respective detectors at exactly the same time, while if the annihilation occurred closer to one detector than the other, the photon would reach the closer detector first. Adding TOF capability improves the statistical quality of the data (i.e., the noise).[7-9] If one could measure the time accurately enough, it would be possible to determine exactly where the photon originated. Unfortunately, current detector and instrumentation technology is not nearly good enough to achieve this level of accuracy. As machines with TOF ability have only recently been introduced, no quality control (QC) or other aspects of such machines are described here.

PET/CT Imaging

The latest trend in PET instrumentation is the addition of a CT system to the PET scanner. In all cases, the manufacturer starts with a state-of-the-art PET scanner, whose characteristics have been described in the section above. The manufacturer then adds a CT system, consisting of a 2-, 4-, 6-, 8-, 16-, 32-, 64-, or greater slice scanner. These combined systems, in practice, demonstrate a range of integration. At one end of the spectrum, the hardware and software of the CT systems are completely integrated within the PET scanner. In this approach, a common, unified gantry is used and a single, unified software system with an integrated PET/CT interface is provided. At the other end of the spectrum, the hardware and software of the CT system are less integrated. In some machines, a separate CT gantry is carefully placed in front of or behind the PET gantry, and a separate workstation is used to control the CT system.

PET Imaging-Attenuation Correction

For dedicated PET scanners, rotating rod sources of germanium-68 (Ge-68)/gallium-68 (Ga-68) or Cesium-137 (Cs-137) are used to acquire a transmission scan for attenuation correction. Typical transmission scans with a rotating rod add about 3-6 minutes to the overall imaging time. This is acceptable for cardiac imaging, but a significant drawback for multi-bed position oncology scans. Since oncology applications have been the driving force behind recent sales of PET scanners, manufacturers looked for a way to reduce this transmission scan time. For this reason, and because of other advantages of CT, nearly all current commercially available PET scanners are hybrid PET/CT systems. These scanners, in general, have eliminated the rotating rod source and instead rely on CT scans for attenuation correction.

CT-based attenuation correction typically adds less than 20 seconds to the scan time of a cardiac scan. The use of either CT or the rotating rod for attenuation correction requires precise alignment between the transmission image and the emission image. An advantage of CT over transmission sources is a much reduced scan time, which helps reduce overall patient motion. The high speed of CT scans, however, freezes the heart at one phase of the respiratory cycle, causing potential misalignment between the CT-based transmission image and the emission data. The latter, of course, are averaged over many respiratory cycles. The respiratory misalignment between the CT image and emission data can produce significant artifacts and errors in apparent uptake at the myocardial segments adjacent to lung tissue.[10] Errors in attenuation correction from misregistration are typically worse if the CT is acquired at full inspiration. At present, software realignment, usually manual, must be performed to minimize this misalignment. Other techniques (e.g., slow CT, respiratory gating, and 4D-CT) are under development for compensating for respiratory motion, but are still in the research phase and are not further described here.

PET AND PET/CT IMAGING QC

PET QC Procedures

The procedures below should be suitable for ensuring overall proper basic operation of a PET scanner. Table 1 lists recommended PET imaging QC

Table 1. Suggested QC procedures: dedicated PET imaging devices

Procedure	Frequency
Acceptance testing (NU 2-2007)	Once upon delivery and upon major hardware upgrades
Daily QC, as recommended by vendor (attenuation blank scan, phantom scan, etc.)	Daily
Sensitivity and overall system performance	Weekly (or at least monthly)
Accuracy (corrections for count losses and randoms)	At least annually
Scatter Fraction	At least annually
Accuracy of attenuation correction	At least annually
Image quality	At least annually
Measurements specified by the manufacturer	As per the manufacturer

schedules. Note that, unlike planar and SPECT imaging, there are no widely accepted, published QC procedures for PET. Some additional procedures may be required by particular manufacturers.

Acceptance testing. It is recommended that the NEMA performance measurements, as defined by NU 2-2007,[5] be made before accepting the PET scanner. Many of these tests can be performed by the company supplying the PET scanner. If so, it is recommended that the purchaser's representative work with the manufacturer's representatives during these tests. The NU 2-2007 recommendations have superseded the NU 2-2001 recommendations.[4] In scope, the tests are nearly equivalent between NU 2-2007 and NU 2-2001, the primary difference being NU 2-2007 addresses the intrinsic radioactivity in LSO and LYSO crystals. For cardiac imaging, these standards should be used rather than NU 2-1994 recommendations,[3] as they better reflect the imaging of objects of the size of a typical adult thorax region by incorporating measurements of the International Electrotechnical Commission (IEC) body phantoms.[11]

There are two reasons for making these performance measurements:

1. To ensure that the new PET scanner meets specifications published by the manufacturer.
2. To provide a standard set of measurements that allows the user to document the limitations of the scanner, and to provide a standard against which to track changes that may occur over time.

Daily QC scan. Each day the PET detectors should be evaluated to ensure proper operation before commencing with patient injections or scans. The daily quality procedure varies according to the design of the scanner and recommendations of the vendor. For example, some scanners utilize an attenuation blank scan to evaluate detector constancy, and others may use a scan of a standard phantom. In addition to numerical output of the scanners software (chi-square, uniformity, etc.), the raw sinogram data also should be inspected to evaluate detector constancy.

Sensitivity. NEMA NU 2-2007 provides recommended procedures for measuring system sensitivity. Subtle changes in PET system sensitivity may occur slowly over time. More dramatic changes in sensitivity may reflect hardware or software malfunction. There are simple tests designed to monitor such changes in sensitivity. Ideally, these tests should be performed weekly, but no less than monthly. For many systems, the daily QC scan also provides a measure useful for tracking changes in sensitivity.

Spatial resolution. Spatial resolution is measured using a point source as specified in the NEMA NU 2-2007 or NEMA NU 2-2001.

Scatter fraction. Intrinsic scatter fraction is measured according to either NEMA NU 2-2007 or NEMA NU 2-2001 specifications.

Accuracy of attenuation correction and overall clinical image quality. Attenuation correction should be assessed using the IEC phantom, as specified in the NU 2-2007 recommendations.[11] If this phantom is not readily available, it is suggested that similar measurements be performed with a phantom approximating a typical human body shape and size (e.g., a 20 by 30-cm elliptical phantom or anthropomorphic phantom). It should have at least one cold sphere or cylinder and one hot sphere or cylinder, as well as at least some material simulating lung tissue to ensure proper performance in the presence of non-uniform attenuating substances.

Variations among manufacturers. The above recommendations regarding PET scanner quality assurance are general guidelines. In addition, each manufacturer has its own periodic QC recommendations for parameters such as ''singles'' sensitivity, coincidence timing, energy calibration, and overall system

performance. These, by necessity, require different measurement protocols that may vary even between models for the same manufacturer. These measurements must be performed as detailed by the manufacturer. However, the measurements specified above are not intended to replace these basic system-specific QC measurements.

CT QC Procedures

The procedures below should be suitable for ensuring overall proper basic operation of a CT scanner. Table 2 lists recommended CT imaging QC schedules. Some additional procedures may be required by particular manufacturers.

Calibration. The reconstructed CT image must exhibit accurate, absolute CT numbers in Hounsfield Units (HU). This is critical for the use of CT images for PET attenuation correction, because the quantitative CT values are transformed, usually via a bilinear or trilinear function with one hinge at or near the CT value for water, to attenuation coefficients at 511 keV. Any errors in CT numbers will be propagated as errors in estimated 511 keV attenuation coefficients, which in turn will adversely affect the attenuation-corrected PET values. CT system calibration is performed with a special calibration phantom that includes inserts of known CT numbers. This calibration is done by the manufacturer's field service engineers. The CT calibration is then checked daily with a water-filled cylinder, usually 24 cm in diameter provided by the manufacturer. In practice, if the error is greater than 5 HU (i.e., different than the anticipated value of 0 HU), the CT system is considered to be out of calibration. The technologist will usually then do an air calibration, to determine if this corrects the overall calibration (i.e., brings the CT number for water back to within 5 HU of 0). If it does not, the manufacturer's field service engineer must be called. On an annual basis, or after any major repair or calibration, calibration is checked by the manufacturer's service engineer.

Field uniformity. The reconstructed CT image must exhibit uniform response throughout the field of view (FOV). In practice, this means that a reconstructed image of a uniform water-filled cylinder must itself demonstrate low variation in CT number throughout this image. In practice, small circular regions of interest (ROIs) are placed at the four corners of the cylinder image, and the mean CT number is compared to that from a region in the center of the phantom; the difference in mean region CT number should not exceed 5 HU. Non-uniformities greater than this may produce sufficient quantitative inaccuracies so as to affect PET attenuation correction based on the CT image.

Table 3 lists recommended CT QC schedules for combined PET/CT Units. Users should consult the manufacturer regarding the specific manner and frequency with which tests should be performed for the CT component of their PET/CT device. Both the American College of Radiology (ACR) and American Association of Physicists in Medicine (AAPM) have published CT testing procedural guidelines.[12,13]

Table 2. CT QC procedures

Test	Requirement	Frequency
Calibration	Mandatory	Monthly*
Field Uniformity	Mandatory	Monthly*

*Or as recommended by the manufacturer.

Combined PET/CT QC Procedures

The PET and CT portion of the combined system should be assessed as described for the dedicated PET and CT imaging devices. In addition to the independent QC tests for the PET and CT portions of the combined system, it is necessary to perform additional tests that assess the combined use of PET and CT. Table 4 lists recommended QC procedures for combined PET/CT units.

Registration. The reconstructed PET and CT images must accurately reflect the same 3D locations (i.e., the two images must be in registration). Such registration is often difficult because the PET and CT portions of all commercial combined PET/CT systems are not coincident (i.e., the PET and CT ''slices'' are not in the same plane) and because the PET and CT gantries are contiguous. In practice, this means that the PET and CT acquisitions do not simultaneously image the same

Table 3. Schedule of CT QC for PET/CT units

Test	Frequency
Water phantom QA	Daily
Tube warm-up	Daily
Air calibration ("fast QA")	Daily
Water phantom checks: slice thickness, accuracy, positioning	Monthly

Table 4. Combined PET/CT QC procedures

Test	Requirement
Registration	Mandatory
Attenuation correction accuracy	Mandatory

slice. In fact, because the bed must travel different distances into the gantry to image the same slice in the patient for PET versus CT, there is ample opportunity for misregistration via x, y, z misalignment of bed motion—or, of perhaps even greater concern, because of differential ''bed sag'' for the PET and CT portions, depending on the table design.

In addition, electronic drift can influence the ''position'' of each image, so that calibrations for mechanical registration can become inaccurate over time. Thus, it is imperative to check PET-to-CT registration on an ongoing basis. This is usually performed with a specific phantom or jig containing an array of point sources visible in both PET and CT.

Errors in co-location in the fused PET-CT images are assessed, such as by means of count profiles generated across transaxial slices. Such errors, after software registration corrections, should be less than 1 mm. It is important to image this registration jig in a number of positions along the bed. It may also be helpful to place a weight on the end of the bed to produce some bed sag and repeat the assessment.

Note: The above considerations are in addition to the patient-specific alignment QC clinically necessary to assess possible patient or respiratory motion (not described here).

Attenuation correction accuracy. The use of the CT image for PET attenuation correction requires a transformation of the observed CT numbers in HU to attenuation coefficients at 511 keV. This transformation is usually accomplished with a bilinear or trilinear calibration curve, with one ''hinge'' at a CT value of 0 (i.e., hinged at the CT value for water).

At a minimum, it is important to image a water-filled cylinder to assess PET field uniformity and PET activity concentrations after CT-based PET attenuation correction. Errors in CT-to-PET attenuation transformations are usually manifest as a corrected PET image without a ''flat'' profile from edge to center (i.e., the activity at the edge is either too high or too low relative to that at the center of the phantom) and with resulting attenuation-corrected absolute PET values that are incorrect (although these values depend on absolute PET scanner calibration as well as accurate CT-based PET attenuation correction).

If possible, the CT-based attenuation-corrected PET values should be compared with those from the rotating rod source-based attenuation-corrected PET values in the same phantom. Moreover, if available, more sophisticated phantoms with variable attenuation and variable activity distributions can be used to more comprehensively assess any errors in CT-based PET attenuation correction.

The accuracy of CT attenuation-corrected PET images is still under investigation.[14] Recent work has reported that even after correcting for potential PET/CT misalignment, tracer uptake maps derived from CT-based attenuation correction differ from those derived using transmission source correction.[10,15,16]

PET ACQUISITION AND PROCESSING PARAMETERS

The acquisition and processing parameters defined in this section apply to both the perfusion and metabolic PET tracers in the sections that follow.

Patient Positioning

Ideally, the patient should be placed in the supine position, with the arms out of the camera FOV. This can be tolerated by nearly all patients, provided that some care is given to a method to support the arms. Alternatively, an overhead bar has often been used as a handhold for arm support. In patients with severe arthritis, whose arms cannot be positioned outside the camera's FOV, cardiac images should be obtained with the patient's arms resting on his/her side. In the latter case, the transmission scan time may have to be increased, and it is of critical importance that the arms do not move between transmission and emission, or artifacts will result. Note that when performing perfusion/metabolism PET studies, it is best to keep the patient positioned similarly for both studies. In patients undergoing PET/CT imaging, arms resting inside the FOV will result in beam-hardening artifacts on the CT-based transmission scan, which usually lead to streak artifact of the corrected emission scans.

Dose Considerations

In determining appropriate patient doses, the following issues should be considered:

1. Staff exposure could be high because of the limited effectiveness of shielding and the potential for large doses (e.g., Rb-82 PET). Thus, standing in close proximity to an Rb-82 generator or the patient during injection should be avoided.
2. Large patients may benefit from higher doses.
3. 3D imaging requires less dosage than 2D imaging due to the improved sensitivity of the system.

Total Counts

The counts per slice necessary to yield adequate quality images will vary from camera to camera depending, in part, on scatter and randoms corrections, as well as the amount of smoothing that is performed. If

one tries to achieve on the order of 7 mm full width at half maximum (FWHM) in-plane resolution and has 10-15% scatter (NEMA), then a typical good-quality study in 2D mode might have on the order of 50,000 true counts per millimeter of transaxial distance over the region of the heart (e.g., for a 4.25-mm slice separation, the counts would be $50{,}000 \times 4.25 = 250{,}000$ counts per slice). These numbers are very approximate and may differ from one scanner to the next. If one is willing to accept a lower resolution (e.g., more smoothing) or more noise, imaging time can be reduced. Since 3D scanners have greater scatter, they usually require more counts than a 2D scanner to achieve the same noise level.

Pixel Size

It is recommended that 2-3 mm per pixel be used. A ''rule of thumb'' in nuclear medicine physics is that one needs at least 3 pixels for every FWHM of resolution in the image. For example, if the data are reconstructed to 8 mm FWHM, then one needs roughly $8 \text{ mm}/3 = 2.7$ mm/pixel. Many institutions achieve a 3 mm sampling rate or better with a 256×256 array over the entire FOV of the camera. Other institutions choose to use a 128×128 array over a limited FOV (e.g., 25-35 cm diameter) centered over the heart, in which case, 2-3 mm/pixel is easy to achieve, cutting out extraneous structures in the FOV, even with a 128×128 array. Either method is acceptable to achieve the desired 2-3 mm/pixel. Greater than 3 mm/pixel may be acceptable for older PET cameras with resolution worse than 1 cm.

Imaging Mode (Static, Gated or Dynamic)

Static PET acquisition produces images that allow relative assessment of tracer uptake on a regional basis. Comparison of regional tracer uptake in relation to the normal tracer distribution is the current standard for the identification regional abnormalities.

Usually, PET tracer counts are sufficiently high to yield good quality ventricular function study. Electrocardiographic (ECG)-gated images are acquired in 8-16 time frames per R to R interval, in a manner similar to SPECT gated perfusion studies but at higher spatial resolution. Given that ventricular contraction and thickening are often clinically useful for assessing viability, gating should be performed when possible. It is important that the gating software does not adversely affect the ungated images (e.g., by loss of counts as a result of beat length rejection). Monitoring the length and number of the accepted beats is critical to assure the accuracy of the gated data. Arrhythmias such as atrial fibrillation, frequent premature ventricular contractions (PVCs), or other abnormal rythms can lead to highly erroneous gated information.

For a dynamic acquisition, PET data are acquired in multiple time sequenced frames. A potential advantage of the dynamic over static acquisition is in the case of patient motion artifact. For example, if a patient should move at the end of the study, one can select and utilize only those dynamic frames with no motion (i.e., summing them together to make one static image). This is easily implemented and takes almost no additional operator time. A more elaborate dynamic acquisition beginning with tracer injection may optionally be used when kinetic analysis over the entire uptake period is to be performed (e.g., compartmental analysis or Patlak analysis). Kinetic analysis permits absolute quantification of the tracer's kinetic properties (e.g., blood flow for Rb-82 and N-13 ammonia, rate of FDG utilization). Performing and interpreting such kinetic analyses can be complex and require expertise.

List mode acquisitions are now available with many new cameras, which enable simultaneous dynamic and ECG-gated acquisitions. This is considered an optional acquisition mode, although it is routinely used by some vendors' processing software.

Image Reconstruction

Several corrections are required for creating data sets that can be used for reconstruction. PET data must be corrected for randoms, scatter, dead time, attenuation, and decay before reconstruction can begin. Once these corrections are applied, the data can be reconstructed with either filtered backprojection (FBP) or iterative algorithms. FBP is the standard method used for reconstruction on older PET systems. FBP images are subject to streak artifacts, especially when the subject is obese or large. This can affect visual analysis but usually does not adversely affect quantitative analysis with regions of interest (i.e., the streaks tend to average out properly over typical volumes of interest). Newer PET/CT systems employ iterative reconstruction methods (e.g., the method of ordered-subsets expectation maximization [OSEM]) yielding images with better noise properties. Although high uptake structures, such as the heart, may not improve their noise characteristics with OSEM, the surrounding lower uptake structures do improve, and streak artifacts are nearly eliminated, thus greatly improving the visual appearance of the image. However, low uptake areas, such as myocardial defects and the left ventricular (LV) cavity at late times, may have slightly or artificially elevated activity levels unless sufficient iterations are performed. It is recommended that one thoroughly characterizes the PET machine and its reconstruction algorithm's behavior with a realistic cardiac phantom.

For rest/stress comparisons, the rest/stress images must have matched resolution. Filtering is usually necessary to achieve adequate noise properties. Care must be taken to match reconstructed resolution when making pixel-by-pixel comparisons of paired myocardial perfusion and metabolism data.

For GSO systems, the images are reconstructed using a row action maximum likelihood algorithm (RAMLA) reconstruction technique, which includes a texture/filter factor. Thus, an additional reconstruction filter should not be performed.

Attenuation Correction

PET cardiac imaging should only be performed with attenuation correction. Attenuation correction can be accomplished with a rotating line source in a dedicated PET system or with CT in a PET/CT system.

For dedicated PET systems, two techniques are typically used for creating the patient-specific transmission maps: direct measurement of patient attenuation with a rotating line source of either Ge-68 or Cs-137 or segmentation of patient-specific attenuation maps. The former are very sensitive to the choice of reconstruction algorithm and, depending on reconstruction algorithm used, could require 60-600 seconds' acquisition time to produce a reasonable attenuation map. Segmentation algorithms are relatively insensitive to noise but are very dependent on the quality of the program used for performing the transmission scan segmentation and are influenced by lung attenuation inhomogeneities (e.g., partial-volume effects from the liver).

Transmission data are typically acquired sequentially, so it is essential that the patient remain still between transmission and emission images. Either pre- or post-scan transmission imaging is satisfactory, providing that the system's software can adequately correct for residual emission activity. Transmission imaging simultaneous with emission imaging is not recommended unless the high count rate and rapidly changing distribution of the emission tracer can be assured to not adversely affect the transmission scan. If the transmission scan is performed at the beginning of the study, attention should be made for potential misregistration with the emission images, possibly due to gradual upward creep of the diaphragm, due to pressure from visceral fat.[17]

For PET/CT systems, x-ray CT can be used for acquiring a transmission map for attenuation correction. An advantage of this approach is the rather rapid (15-30 seconds) acquisition of the transmission map, which can be repeated for each imaging session, rest and stress perfusion studies as well as for subsequent metabolic imaging, if necessary. The CT scan can be reviewed for additional, independent diagnostic information, such as coronary calcium visualization and other extra-cardiac anatomic information. To acquire a CT-based transmission scan, it is necessary to first acquire a planar scout CT acquisition. This scan is used to measure the axial limits of the CT acquisition. Following this acquisition, the CT transmission scan is acquired. The best approach for CT transmission imaging is still evolving, and therefore this guideline can only suggest some considerations. Some of the considerations for CT scanning are as follows (Table 5):

1. If CT is used for either attenuation correction or anatomical evaluation, this will have an effect on the kV and mAs used in the acquisition. A transmission

Table 5. General guidelines for CT-based transmission imaging

CT parameter	General principle	Effect on patient dose
Slice collimation	Should approximate the slice thickness of PET (eg., 4–5 min.)	No effect
Gantry rotation speed	Slower rotation speed helps blur cardiac motion (eg., 1 sec/revolution or slower)	Slower gantry rotation increases radiation
Table feed per gantry rotation(pitch)	Relatively high pitch(eg., 1:1)	Inversely related to pitch
ECG gating	ECG gating is not recommended	Decreases without ECG gating
Tube potential	80–140 kVp, depending on manufacturer specification	Increases with higher kVp
Tube current	Because the scan is only acquired for AC, low tube current is preferred (10–20 mA)	Increases with higher mA
Breathing instructions	End-expiration breathhold or shallow free-breathing is preferred (see text)	No effect
Reconstructed slice thickness	Should approximate the slice thickness of PET (eg., 4–5 mm)	No effect

scan usually requires only a low CT current, as opposed to calcium scoring or CT angiography, which require higher CT currents.

2. Breathing protocols are not clearly settled. Recent data suggest that respiratory averaging may be a useful method of reducing breathing related artifacts. Other methods, such as free breathing with a slow CT scan or ultra-rapid CT acquisition (depending on the CT device available) have also been proposed. Current practice discourages breath-holding, particularly in end-inspiration because of the potential for it to cause uncorrectable misregistration. A transmission CT scan performed at the same speed as for whole-body PET/CT images frequently produces artifacts at the lung-liver interface and can sample parts of the heart and diaphragm in different positions, causing misregistration and an artifact where pieces of the diaphragm appear to be suspended in the lung. Although specifics vary among laboratories, the duration of the CT transmission scan is typically from 10-30 seconds. CT attenuation correction with 64 slice devices can achieve an ultra-rapid CT in 1.5 seconds, which appears to reduce such CT artifacts. Therefore, it is imperative to ensure proper registration between transmission and emission data for quality assurance and proper interpretation of PET images. Several approaches are currently being devised to reduce misregistration artifacts, such as reducing CT tube current and increasing the duration CT acquisition to better match the temporal resolution between the attenuation and emission maps.[18,19]
3. Metal artifacts[20] can present a challenge for the reconstruction algorithm and must be compensated for to produce accurate attenuation maps.[21,22]
4. Ideally, stress transmission images should be acquired during peak stress or vasodilation, which is not practical. As such, the technologist and physician must carefully inspect the transmission and emission data sets to ensure that they are properly registered in the transaxial, sagittal, and coronal planes. For patients undergoing PET/CT, a separate CT-based transmission scan for correction of the stress images is standard. For Rb-82, a post-stress transmission scan is preferred to minimize misregistration artifacts on the corrected Rb-82 images when misregistration compensation software is not available.

PET MYOCARDIAL PERFUSION IMAGING

The goal of evaluating myocardial perfusion with PET imaging is to detect physiologically significant coronary artery narrowing with a view towards aggressive risk factor modification in order to:

1. Delay or reverse the progression of atherosclerosis.
2. Alleviate symptoms of ischemia by medical or revascularization therapy.
3. Prevent future adverse events.
4. Improve patient survival.

Stress and rest paired myocardial perfusion studies are commonly performed to assess myocardial ischemia and/or infarction. Current Food and Drug Administration (FDA)-approved and Centers for Medicare & Medicaid Services (CMS)-reimbursable PET myocardial blood flow tracers are limited to Rb-82 and N-13 ammonia. Normal myocardial perfusion on stress imaging implies absence of physiologically significant coronary artery disease (CAD). Abnormal myocardial perfusion on stress imaging suggests the presence of significantly narrowed coronary arteries. If the stress-induced regional perfusion defect persists on the corresponding paired rest images, it suggests the presence of an irreversible myocardial injury. On the other hand, if the defect on the stress images resolves completely or partially on the rest images, it suggests the presence of stress induced myocardial ischemia. Imaging of myocardial perfusion can also be combined with myocardial metabolism imaging with F-18 FDG for the assessment of myocardial viability in areas of resting hypoperfusion and dysfunctional myocardium.

Patient Preparation

Patient preparation is similar to preparation for stress and rest myocardial SPECT imaging. This includes an overnight fast of 6 hours or more, with the exception of water intake. Patients should avoid caffeinated beverages for at least 12 hours, and avoid theophylline-containing medications for at least 48 hours.[23]

Cardiac Stress Testing

Details of pharmacologic or exercise stress testing are beyond the goals of this document. Nonetheless, stress protocols are, for the most part, generic for all perfusion agents.[23] The specific differences in acquisition protocols for Rb-82 and N-13 ammonia imaging are related to the duration of uptake and clearance of these radiopharmaceuticals and their physical half-lives. No data are available yet with PET and the newly approved A2A selective adenosine receptor agonist, Regadenoson.

Rb-82 Perfusion Imaging

Tracer properties. Rb-82 PET myocardial perfusion imaging is a well established and highly accurate

technique for detecting hemodynamically significant CAD.[14,24,25] Rb-82 is a monovalent cationic analog of potassium. It is produced in a commercially available generator by decay from strontium-82 (Sr-82) attached to an elution column. Sr-82 has a half-life of 25.5 days and decays to Rb-82 by electron capture. Rb-82 decays with a physical half-life of 75 seconds by emission of several possible positrons, predominantly of very high energy. The resulting long positron range slightly worsens image resolution compared to F-18 and N-13. The daughter product is krypton-82, which is stable. The Sr-82-containing generator is commercially available and is replaced every 4 weeks, thus obviating the need for a cyclotron.

Rb-82 is eluted from the generator with 10 to 50 mL normal saline by a computer-controlled elution pump, connected by intravenous (IV) tubing to the patient. While the generator is fully replenished every 10 minutes, experiments have shown that 90% of maximal available activity can be obtained within 5 minutes after the last elution. Thus, serial imaging can be performed every 5-6 minutes. While the short half-life of Rb-82 challenges the performance limits of PET scanners, it facilitates the rapid completion of a series of resting and stress myocardial perfusion studies.

Rb-82 is extracted from plasma with high efficiency by myocardial cells via the Na^+/K^+ adenosine triphosphatase pump. Its extraction is less than N-13 ammonia, and extraction decreases with increasing blood flow. Rb-82 extraction can be decreased by severe acidosis, hypoxia, and ischemia.[26-28] Thus, while uptake of Rb-82 predominantly depends on myocardial blood flow, it may be modulated by metabolism and cell integrity.

Dosimetry. The radiation dosimetry from Rb-82 in an adult may vary from 1.75 to 7.5 mSv total effective dose for a maximal allowable activity of 60 mCi at both rest and stress.[29] With current advances in PET instrumentation, diagnostic quality PET images can be acquired using only 20-40 mCi of Rb-82 for each of the rest and stress phases of the study. As a result, the effective dose of radiation exposure from Rb-82 PET can be halved.

Acquisition parameters. Acquisition parameters for different types of PET scanners are shown in Tables 6 and 7. The short half-life of Rb-82 poses a challenge for achieving optimal image quality. As such, optimal acquisition parameters differ among the several main types of PET scanners. Because of the short half-life of Rb-82 and the need for the patient to lie still in the camera during the study, stress imaging of this agent is primarily limited to pharmacologic stress, although

Table 6. Rb-82 rest/stress myocardial perfusion imaging guideline for BGO and LSO (LYSO) PET imaging systems

Feature	BGO Systems	LSO (LYSO) Systems	Technique
Stress testing	Pharmacologic agents		Standard
Tracer Dose			
2D Scanner	40–60 mCi (1480–2220 MBq)		Standard
3D Scanner	10–20 mCi (370–740 MBq)	30–40 mCi (1110–1480 MBq)	Standard
Injection rate	Bolus of ≤30 seconds		Standard
Imaging delay after injection	LVEF > 50%: 70–90 seconds		Acceptable
	LVEF < 50% or unknown: 90–130 seconds		
	List mode: acquire immediately		
Patient positioning			
PET	Use scout scan: 10–20 mCi Rb-82 (370–740 MBq)		Standard
	Use transmission scan		Optional
PET/CT	CT scout		Standard
Imaging mode	List mode: gated/dynamic (no delay after injection)		Preferred
	Gated acquisition (delay after injection)		Optional
Imaging duration	3–6 minutes		Standard
	3–10 minutes		Optional
Attenuation correction	Measured attenuation correction, before or after		Standard
Reconstruction method	FBP or iterative expectation maximization (e.g., OSEM)		Standard
Reconstruction filter	Sufficient to achieve desired resolution/smoothing, matched stress to rest		Standard
Reconstructed pixel size	2–3 mm		Preferred

Table 7. Rb-82 rest/stress myocardial perfusion imaging guideline for GSO PET imaging systems

Feature	GSO Systems	Technique
Stress testing	Pharmacologic agents	Standard
Tracer dose (3D)	20 mCi (740 MBq)	Standard
Injection rate	Bolus of $\leq$ 30 seconds	Standard
Imaging delay after injection	LVEF $>$ 50%: 70–90 seconds	Standard
	LVEF $<$ 50% or unknown: 90–130 seconds	
	List mode: acquire immediately	
	Longer delays than the above must be used if count rate at these times exceeds the maximum value specified by the manufacturer	
Patient positioning		
PET	Use scout scan: 10–20 mCi Rb-82 (370–740 MBq)	Standard
	Use transmission scan	Optional
PET/CT	CT scout	Standard
Imaging mode	List mode: gated/dynamic (no delay after injection)	Standard
Imaging duration	3–6 minutes	Standard
	3–10 minutes	Optional
Attenuation correction	Measured attenuation correction, before or after	Standard
Reconstruction method	Iterative (RAMLA)	Standard
Reconstruction filter	None	Standard
Reconstructed pixel size	4 mm	Standard

reasonable Rb-82 images have also been obtained with supine bicycle and treadmill exercise.[30,31]

Scout scanning. Scout scanning is recommended before each injection to ensure that the patient is correctly positioned and is not exposed to unnecessary radiation. This can be done with a fast transmission image or with a low-dose Rb-82 injection (10-20 mCi). Note that the low-dose Rb-82 scout scan is also used to estimate circulation times and cardiac blood pool clearance times, which assist in selection of the optimum injection to imaging delay time between Rb-82 injection and initiation of acquisition of myocardial Rb-82 images. With PET/CT systems, a low dose CT scout scan is routinely used for patient positioning.

Imaging parameters. Rest imaging should be performed before stress imaging to reduce the impact of residual stress effects (e.g., stunning and steal). For Rb-82, about 80% of the useful counts are acquired in the first 3 minutes, 95% of the useful counts are obtained in the first 5 minutes, and 97% are obtained in the first 6 minutes. The patient should be infused with Rb-82 for a maximum of 30 seconds. After the dose is delivered, patients with normal ventricular function, or left ventricular ejection fraction (LVEF) $>$ 50%, are typically imaged starting 70-90 seconds after the injection. For those with reduced ventricular function, or LVEF 30-50%, imaging usually is begun 90-110 seconds after termination of the infusion. Those with poor function, or LVEF $<$ 30%, are typically imaged at 110-130 seconds. Excessive blood pool counts can scatter into myocardial counts, impacting defect size and severity. Excessive blood pool counts can also make the left ventricular cavity appear smaller, especially at rest, leading to a false perception of LV cavity dilatation during stress. These delay times are applicable for both static and ECG gated acquired images.

N-13 Ammonia Perfusion Imaging

N-13 ammonia is a valuable agent for measuring either absolute or relative myocardial blood flow.[32,33] For measurements of absolute blood flow, dynamic acquisition from time of injection is required, followed by applying 2- and 3-compartment kinetic models that incorporate both extraction and retention rate constants. Absolute flow measurements with ammonia are

performed primarily in research settings, require a high level of expertise, and are not commercially available. In a clinical setting, ammonia PET images are assessed visually or semi-quantitatively for the evaluation of regional myocardial perfusion defects or for the determination of myocardial viability.[34-36]

N-13 ammonia is an extractable myocardial perfusion tracer that has been used extensively in scientific investigations with PET over the past two decades. At physiologic pH, ammonia is in its cationic form with a physical half-life of 10 minutes. Its relatively short half-life requires an on-site cyclotron and radiochemistry synthesis capability. The N-13 nitrogen decays by positron emission. The daughter product is C-13 carbon, which is stable. Myocardial uptake of N-13 ammonia depends on flow, extraction, and retention. First-pass myocardial extraction of N-13 ammonia is related inversely and nonlinearly to blood flow.[37] Following this initial extraction across the capillary membrane, ammonia may cross myocardial cell membranes by passive diffusion or as ammonium ion by the active sodium-potassium transport mechanism. Once in the myocyte, N-13 ammonia is either incorporated into the amino acid pool as N-13 glutamine or back-diffuses into the blood. The myocardial tissue retention of ammonia as N-13 glutamine is mediated by adenosine triphosphate and glutamine synthetase. Thus uptake and retention can both be altered by changes in the metabolic state of the myocardium although the magnitude of metabolic effects on the radiotracer retention appears to be small.

Dosimetry. The radiation dosimetry from N-13 ammonia in an adult is 1.48 mSv total effective dose from 20 mCi.[38] The critical organ is the urinary bladder, which receives 6 mSv from 20 mCi.[39] The dosimetry is relatively low, due to the short half-life of N-13 and the low energy of the emitted positrons.

Acquisition parameters. Table 8 summarizes the recommended guidelines for performing N-13 ammonia perfusion scans with dedicated, multicrystal PET or PET/CT cameras for rest and stress myocardial PET perfusion imaging for the diagnosis and evaluation of CAD, or as part of an assessment of myocardial viability.

Dose. Typically, 10-20 mCi of N-13 ammonia is injected. Large patients may benefit from higher, or 25-30 mCi, doses. In addition, the dose of radioactivity administered will also depend on whether images are obtained in 2D or 3D imaging mode.

PET METABOLIC IMAGING

PET Glucose Metabolism

For a given physiologic environment, the heart consumes the most efficient metabolic fuel as an adaptive response to meet its energy demands. Under fasting and aerobic conditions, long-chain fatty acids are the preferred fuel in the heart as they supply 65-70% of the energy for the working heart, and some 15-20% of the total energy supply comes from glucose.[40] However, the myocardium can use various other metabolic

Table 8. N-13 ammonia cardiac perfusion studies

Feature		Technique
Stress testing	Pharmacologic agents	Standard
Tracer dose (2D or 3D)	10–20 mCi (typical) (370–740 MBq)	Standard
Injection rate	Bolus or <30 seconds infusion	Preferred
Imaging delay after injection	1.5–3 minutes after end of infusion	Standard
Patient positioning		
PET	Use scout scan: 1–2 mCi (37–74 MBq)	Optional
	Use transmission scan	Standard
PET/CT	CT Scout Scan	Standard
Imaging mode	ECG gating of myocardium	Preferred
	Static or list mode	Optional
	Dynamic	Optional
Imaging duration	10–15 min	Standard
Attenuation correction	Measured attenuation correction, before or after	Standard
Reconstruction method	FBP or iterative expectation maximization (e.g., OSEM)	Standard
Reconstruction filter	Sufficient to achieve desired resolution/smoothing, matched stress to rest	Standard
Reconstructed pixel size	2–3 mm	Preferred
	4 mm	Optional

substrates depending on substrate availability, hormonal status, and other factors.[41,42]

Metabolic adaptation to changes in regional blood flow or other triggers is an essential component of maintaining normal cardiac function. Acute and chronic metabolic adaptation to a temporary or sustained reduction in coronary blood flow is in place to protect the structural and functional integrity of the myocardium. Reversible metabolic changes, as an adaptive measure to sustain myocardial viability, will occur in the setting of diminished, but not absent, regional myocardial blood flow. When myocardial blood flow is absent, irreversible metabolic changes will occur followed by myocardial infarction and cell death.

The breakdown of fatty acids in the mitochondria via beta-oxidation is exquisitely sensitive to oxygen deprivation. Therefore, in the setting of reduced oxygen supply, the myocytes compensate for the loss of oxidative potential by shifting toward greater utilization of glucose to generate high-energy phosphates. An acute switch from aerobic to anaerobic metabolism may be a necessary prerequisite for immediate cell survival following acute myocardial ischemia. Without these acute adaptive changes in metabolism, the resulting energy deficit leads to cell death.

Tracers of myocardial metabolism such as carbon-11 labeled fatty acids, acetate, or glucose, will not be covered in this document, due to their current investigational status and lack of FDA approval.

F-18 FDG Metabolism Imaging

Tracer properties. The principal radiopharmaceutical in clinical cardiac PET myocardial viability imaging is F-18 FDG, which is an analog of glucose and is used to image myocardial glucose utilization in vivo. CMS has approved reimbursement of FDG for the evaluation of myocardial viability.

The F-18 radiolabel is produced in a cyclotron through the (p,n) reaction, consisting of bombardment of O-18 enriched water.[43] F-18 decays by the emission of a positron with a half-life of $\sim$110 minutes. The low kinetic energy of the positron, 635 keV, allows the highest spatial resolution among all PET radionuclides. The 110-minute physical half-life of FDG allows sufficient time for synthesis and purification, its commercial distribution in a radius of several hours from the production site, its temporary storage at the user site, the absorption time after injection, and sufficient imaging time to yield images of high quality.

FDG enters myocardial cells by the same transport mechanism as glucose. Once in the cell, it is phosphorylated by hexokinase to FDG-6-phosphate. Once phosphorylated, subsequent metabolism of FDG is minimal. Because the dephosphorylation rate of FDG is slow, it becomes essentially trapped in the myocardium, allowing adequate time to image regional glucose uptake by PET. Following IV injection of 5-15 mCi of FDG, imaging can commence either immediately during the infusion of the radiotracer, if quantification of glucose metabolic rates is desired, or about 45-90 minutes after the injection of the radiotracer, if only qualitative assessment of the relative distribution of the radiotracer in the LV myocardium is needed.

Tracer dosimetry. The whole body dosimetry from a 10-mCi dose is 7 mSv.[44] For FDG, the critical organ is the urinary bladder, which receives 59 mSv.

Patient preparation. There are several approaches to stimulate myocardial glucose metabolism with either oral or IV glucose loading. Tables 9, 10, and 11 summarize the recommended guidelines for performing cardiac FDG scans with dedicated, multicrystal PET and PET/CT cameras, as part of an assessment of myocardial viability. Tables 10 and 11 summarize the patient preparation and method of FDG administration. Table 12 discusses the image acquisition.

Myocardial substrate utilization. For the evaluation of myocardial viability with FDG, the substrate and hormonal levels in the blood need to favor utilization of glucose over fatty acids by the myocardium.[40,42,45] This is usually accomplished by loading the patient with glucose after a fasting period of at least 6 hours to induce an endogenous insulin response. The temporary increase in plasma glucose levels stimulates pancreatic insulin production, which in turn reduces plasma fatty acid levels through its lipogeneic effects of adipocytes and also normalizes plasma glucose levels. The most common method of glucose loading is with an oral load of 25-100 g, but IV loading is also used. The IV route avoids potential problems due to variable gastrointestinal absorption times or inability to tolerate oral dosage. Because of its simplicity, most laboratories utilize the oral glucose-loading approach, with supplemental insulin administered as needed. The physician should take into account whether or not the patient is taking medications that may either antagonize or potentiate the effects of insulin.

Diabetic patients. Diabetic patients pose a challenge, either because they have limited ability to produce endogenous insulin or because their cells are less able to respond to insulin stimulation. For this reason, the simple fasting/oral glucose-loading paradigm is often not effective in diabetic patients. Use of insulin along with close monitoring of blood glucose (Table 10) yields satisfactory results. Improved FDG images can also be seen when image acquisition is delayed 2-3 hours after injection of the FDG dose. Of course, the latter comes at the expense of increased decay of the radiopharmaceutical. An alternative technique is the euglycemic hyperinsulinemic clamp, which is a rigorous and time-consuming

Table 9. FDG cardiac PET: patient preparation guidelines—an overview

Procedure		Technique
Fasting period	*Step 1*: Fast patient	
	6–12 hours	Preferred
	<6 hours	Suboptimal
	Step 2: Check blood glucose (BG) and then glucose load (choose one of the following 4 options)	
Oral glucose load	*Option 1*: Oral glucose loading	
	IF: fasting BG < ~250 mg/dL (13.9 mmol/L)	Standard
	THEN: (1) Oral glucose load: typically 25–100 g orally (see Table 10)	
	(2) Monitor BG (see Table 10)	
	IF: fasting BG > ~250 mg/dL (13.9 mmol/L)	Standard
	THEN: See Table 10	
	OR	
IV, protocol A	*Option 2*: Dextrose IV infusion	Optional
	For details, see sample protocol A (appendix 1)	
	OR	
IV, protocol B	*Option 3*: Dextrose IV infusion	Optional
	For details, see sample protocol B (appendix 2)	
	OR	
Acipimox	*Option 4*: Acipimox	
	Acipimox, 250 mg orally, not available in United States	
	Step 3: Administer FDG	
FDG injection	Time: Dependent on which option was selected	Standard
	Administer FDG intravenously; see Table 11, item 1, for details	
	Step 4: Begin imaging	
Begin PET imaging	Time 0–90 minutes post FDG injection: start imaging, see Table 11	

Table 10. Guidelines for blood glucose maintenance (e.g., after oral glucose administration) for optimal FDG cardiac uptake, blood glucose of approximately 100-140 mg/dL (5.55-7.77 mmol/L) at FDG injection time

BG at 45–60 min after administration	Possible restorative measure	Technique
130–140 mg/dL (7.22–7.78 mmol/L)	1 u regular insulin IV	Standard
140–160 mg/dL (7.78–8.89 mmol/L)	2 u regular insulin IV	
160–180 mg/dL (8.89–10 mmol/L)	3 u regular insulin IV	
180–200 mg/dL (10–11.11 mmol/L)	5 u regular insulin IV	
>200 mg/dL (>11.11 mmol/L)	Notify physician	

procedure.[46,47] However, it allows close titration of the metabolic substrates and insulin levels, which results in excellent image quality in most patients. Shorter IV glucose/insulin-loading procedures of 30 minutes have also been used with some success (see Protocol A, Appendix 1 and Protocol B, Appendix 2).[48]

While some have advocated performing FDG viability scans under fasting conditions, it is recommended that they be performed under glucose loaded conditions. This maximizes FDG uptake in the myocardium, results in superior image quality, and reduces the regional variations in FDG uptake

Table 11. FDG cardiac PET: acquisition guidelines for dedicated, multicrystal PET scanner

Feature		Technique
Tracer dose (2D or 3D)	5–15 mCi (185–555 MBq)	Standard
Injection rate	Not critical, bolus to 2 minutes	Standard
Image delay after injection	45–60 min after injection (keep constant for repeat studies)	Standard
Patient positioning		
PET	Use an FDG scout scan	Optional
	Use transmission scan	Standard
PET/CT	CT Scout Scan	Standard
Imaging mode	2D or 3D	Standard
	Static or list mode	Standard
	Dynamic	Optional
Image duration	10–30 min (depending on count rate and dose)	
Attenuation Correction	Measured attenuation correction: before or immediately after scan	Standard
Reconstruction method	FBP or iterative expectation maximization (e.g., OSEM)	Standard
Reconstruction filter	Sufficient to achieve desired resolution/smoothing, matched between consecutive studies	Standard
Reconstructed pixel size	2–3 mm	Preferred
	4–5 mm	Acceptable

Note: If metabolism imaging is combined with PET perfusion imaging, the same parameters for patient positioning, attenuation correction, and image reconstruction should be applied.

Table 12. Semiquantitative scoring system of defect severity and extent

Grade	Interpretation	Score
Normal counts	Normal perfusion	0
Mild reduction in counts	Mildly abnormal	1
Moderate reduction in counts	Definitely abnormal	2
Severe reduction in counts	Definitely abnormal	3
Absent counts	Definitely abnormal	4

that can occur when imaging under fasting conditions.[49]

Acipimox. Acipimox is a nicotinic acid derivative, which is not FDA approved in the United States. It has been used successfully in Europe instead of glucose loading. Acipimox inhibits peripheral lipolysis, reduces plasma free fatty acid levels, and stimulates myocardial glucose utilization.[48,50]

Acquisition parameters. Acquisition parameters for PET cardiac FDG imaging are itemized in Table 11 and its accompanying notes. If FDG PET metabolic images are being compared to perfusion images acquired by SPECT, the interpreter should be mindful that there will be differences in soft tissue attenuation, image resolution, and registration problems of images acquired on different instruments. It should be noted that if a Tl-201 or Tc-99m-labeled perfusion tracer is used to assess myocardial perfusion, there is no need to delay the FDG PET images, from an instrumentation point of view, if the 2D PET acquisition mode is applied. The relatively lower photons emitted from Tl-201 and Tc-99m will not interfere with the higher energy F-18 photons. However, with 3D PET imaging, the Tc-99m activity can increase dead time and thus decrease the ''true'' counts from the FDG. If FDG PET images are acquired first, then it is necessary to wait at least 15 or more half-lives, depending on the dose of F-18 administered, before a low-energy (e.g., Tl-201 or Tc-99m) SPECT study is performed. This is because the 511 keV photons from the PET tracers easily penetrate the collimators that are commonly used for Tl-201 or Tc-99m imaging.

Dose. Typically, 5-15 mCi is injected in a peripheral vein (see counts requirements below). Injection speed is not critical (i.e., bolus to 2 minutes). To reduce patient dose to the bladder, patients should be encouraged to void frequently for 3-4 hours after the study.

Scan start time and duration. Wait a minimum of 45 minutes before starting the static FDG scan acquisition. Myocardial uptake of FDG may continue to increase, and blood pool activity to decrease, even after 45 minutes. While waiting 90 minutes after the injection of FDG may give better blood pool clearance and myocardial uptake, especially in diabetics or subjects with high blood glucose levels, this comes at the expense of reduced count rate. Scan duration is typically 10-30 minutes. If acquired in 3D mode, compared with 2D mode with the same machine, a smaller dose is typically required to achieve the same total count rate, but the imaging time may or may not be reduced as a result of count rate limitations and increased scatter. In some PET cameras, beyond a certain dose, the 3D mode will actually produce poorer-quality images for the same dose and imaging time than 2D mode. For this reason, it is critical to have fully characterized the performance of the PET system.

IMAGE DISPLAY, NORMALIZATION, AND EVALUATION FOR TECHNICAL ERRORS

Recommendations for display of PET perfusion rest-stress and/or perfusion-metabolism images are consistent with those listed in previous guidelines for SPECT myocardial rest-stress perfusion imaging.[51] It is necessary to examine the transaxial, coronal, and sagittal views for assessing the alignment of the emission images acquired during stress, rest, and metabolism, as well as the transmission images. Fused transmission and emission images are preferred. Images that are not aligned (e.g., due to patient or cardiac motion) may cause serious image artifacts, especially when only one set of attenuation correction images has been applied to all emission images for attenuation correction. This is particularly a problem when CT is used for attenuation correction.[16] It is important that the fusion images be reviewed for potential misalignment problems and appropriate adjustments be made. Some vendors' systems now provide software that allows realignment of transmission CT and emission PET images before processing, and in other instances image data can be transferred to a stand-alone PC that has realignment software.

The reoriented images should be displayed as follows:

1. A short-axis view, by slicing perpendicular to the long axis of the LV from apex (left) to base (right).
2. A vertical long-axis view, by slicing vertically from septum (left) to lateral wall (right).
3. A horizontal long-axis view, by slicing from the inferior (left) to the anterior wall (right).

For interpretation and comparison of perfusion and metabolism images, slices of all data sets should be displayed aligned and adjacent to each other. In the absence of motion artifact, combined assessment of perfusion and metabolism within a single PET session offers the advantage of copying the ventricular long axis defined during image orientation from one image set to the second set, thereby optimizing the matching of the perfusion with the metabolism images. Normalization of the stress and rest perfusion image set is commonly performed by using the maximal myocardial pixel value in each of the two or three image sets; or, for example, the average pixel value with the highest 5% of activity of the perfusion images. Each perfusion study is then normalized to its own maximum.

The metabolism images are normalized to the counts in the same myocardial region on the resting perfusion images (e.g., with the highest count rates that were obtained on the perfusion study).[52,53] An important limitation of this approach, however, is that glucose metabolism may be enhanced or abnormally increased in regions with ''apparently'' normal resting myocardial perfusion, if such regions are subtended by significantly narrowed coronary arteries and are in fact ischemic on stress myocardial perfusion studies.[54] Moreover, visual assessment of resting myocardial uptake of the radiotracer reflects the distribution of myocardial blood flow in ''relative'' terms (i.e., relative to other regions of the LV myocardium) and not in ''absolute'' terms (i.e., mL/min/gm myocardial tissue). Thus, in some patients with multivessel CAD, it is possible that all myocardial regions are in fact hypoperfused at rest in ''absolute'' terms (i.e., termed balanced reduction in blood flow) yet appear normal in ''relative'' terms. If stress images of PET are available, it is recommended that the normal reference region on stress perfusion images be used for normalizing FDG PET images.[35] In the presence of left bundle-branch block (LBBB), where the septal FDG uptake is spuriously decreased, the septum should not be used as the site for normalization. Accordingly, the ECG should be reviewed in conjunction with perfusion/viability imaging.

Standard Segmentation and Polar Map Display

Standard segmentation model divides the LV into three major short-axis slices: apical, mid-cavity, and basal. The apical short-axis slice is divided into four

segments, whereas the mid-cavity and basal slices are divided into six segments. The apex is analyzed separately, usually from a vertical long-axis slice. Although the anatomy of coronary arteries may vary in individual patients, the anterior, septal, and apical segments are usually ascribed to the left anterior descending coronary artery, the inferior and basal septal segments to the right coronary artery, and the lateral segments to the left circumflex coronary artery. The apex can also be supplied by the right coronary and left circumflex artery. Data from the individual short-axis tomograms can be combined to create a polar map display, representing a 2D compilation of all the 3D short-axis perfusion data. Standard 17 segments in the polar map are displayed in Figure 1.[55] The 2D compilation of perfusion and metabolism data can then easily be assigned to specific vascular territories. These derivative polar maps should not be considered a substitute for the examination of the standard short-axis and long-axis cardiac tomographic slices.

3D Display

If suitable software is available, reconstructed myocardial perfusion and metabolism data sets can be displayed in a 3D static or cine mode, which may be convenient for morphologic correlation with angiographic correlation derived from CT, magnetic resonance, or conventional angiography. Some of the software may allow the overlay the coronary anatomy on the 3D reconstructed perfusion and metabolism images of the heart. Currently, an advantage of 3D over conventional 2D displays with regard to accuracy of PET image interpretation has not been demonstrated.

Recommended Medium for Display

It is strongly recommended for the interpreting physician to use the computer monitor rather than film hard copies for interpretation of myocardial perfusion and metabolism images. The latter would be especially important for gated PET images, where dynamic wall motion data is viewed for proper interpretation of regional abnormalities. A linear gray scale, monochromatic color scale, or multicolor scale can be used as the type of display, depending on user experience and preference.

Image Evaluation for Technical Sources of Errors

Patient motion. PET images are typically generated with nonmoving circular arrays of scintillation detectors that acquire all projection data simultaneously. In contrast to SPECT imaging with rotating gamma cameras, in which patient motion leads to a typical misalignment between adjacent projection images and can be identified by viewing a projection movie. Movement during static PET imaging affects all projections and is therefore more difficult to identify. Substantial patient motion can produce blurring of image contours. Therefore, attention to patient motion during image acquisition is essential to minimize motion artifacts.

Patient positioning before and immediately after image acquisition should be carefully evaluated (e.g., by checking the alignment of the camera's positioning laser beams with ink markers on the patient's skin). Acquisition of a brief scan or scout image after injection of a

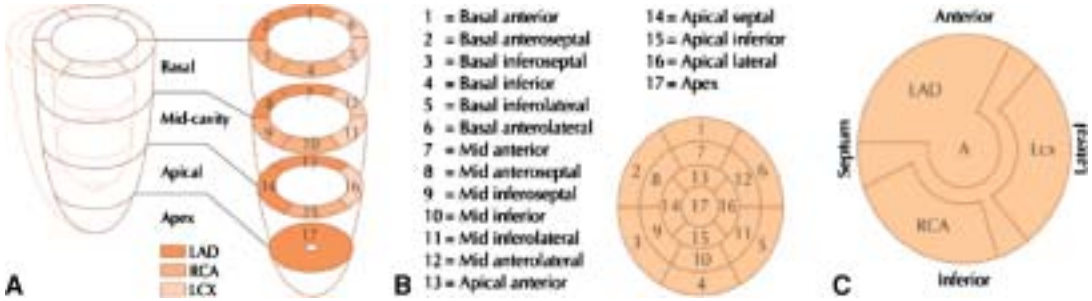

Figure 1. LV Myocardial segmentation, standard nomenclature, and vascular territories. PET images are interpreted on the basis of the presence, location, extent, and severity of myocardial perfusion and metabolic defects using a standard 17-segment model and visual scoring. **A** The standard segmentation model divides the LV into three major short-axis slices: apical, midcavity, and basal. The apical short-axis slice is divided into four segments, whereas the mid-cavity and basal slices are divided into six segments. The apex is analyzed separately, usually from a vertical long-axis slice. **B** Data from the individual short-axis tomograms can be combined to create a polar map plot, representing a 2D compilation of all the 3D short-axis perfusion data. Standard nomenclature for the 17 segments is outlined. **C** The 2D compilation of perfusion data can then easily be assigned to specific vascular territories. (*From* Dilsizian V.; *Reprinted with permission*)[55].

small dose, usually one-third of the standard dose of Rb-82, may facilitate accurate patient positioning. With PET/CT systems, a CT scout scan (10 mA) is routinely used for accurate patient positioning. In instances of patient discomfort and likely patient motion, especially during longer image acquisition times, one approach to reduce adverse effects of motion is to acquire a series of 3-4 sequential image frames instead of a single static image of longer duration. Dynamic imaging would also be effective for this purpose. If the quality of one of the serially acquired frames is compromised by motion, then that frame can be rejected and only frames that are of acceptable quality and are free of motion artifacts are summed for the final image analysis.

Attenuation correction. Correction of the emission images for photon attenuation is critical for cardiac PET imaging. Positron-emitting tracers are more sensitive to attenuation artifacts than single photons. Coincidence detection systems must detect both simultaneously emitted photons. As each of the two photons is susceptible to tissue attenuation, attenuation artifacts are generally greater. Therefore, only attenuation-corrected images should be used for clinical interpretation. Potential sources of errors include misalignment between emission and transmission data resulting from patient motion. Misalignments of 1.5-2 cm, for example, can lead to as much as a 30% change in the observed regional myocardial radioactivity.[10,16,17,56]

Vertical and transaxial displacement of the heart can occur even in the absence of movement of the chest. The latter is perhaps related to the change of breathing pattern, which may occur during pharmacologic stress. This could be thought as analogous to the ''upward creep'' phenomenon seen in SPECT imaging. As a result, under-correction artifacts due to the lower attenuation coefficient of the overlapping lung tissue may appear in the anterior or anterolateral regions, or over-correction artifacts due to the higher attenuation coefficients of the overlapping subdiaphragmatic tissues may appear in the inferior region as ''hot spots.'' Inspection of fused emission-transmission images for possible misalignment is essential because the resulting artifacts would greatly affect image interpretation. Fused images should be inspected in the axial (lateral displacement), coronal (vertical displacement) and sagittal (vertical displacement) slices. Alternatively, displacement can be detected on transaxial images by counting the number of pixels by which the cardiac image is displaced between resting and stress transaxial acquisitions. Identification of vertical and lateral displacements that result in misalignment between the emission and transmission images is relatively straightforward.

The degree of co-registration of transmission and emission images should be carefully examined using the fusion software available on integrated PET/CT systems to assess the reliability of images with attenuation correction. If there is patient motion and the cardiac silhouette does not superimpose perfectly on the transmission and emission images, the images without attenuation correction need to be examined as well. In general, vertical misalignment is easier to resolve by offsetting the alignment between the emission and transmission scans, but this option is not generally available.

When the transmission maps are acquired using CT, the incidental findings in the portion of the chest in the FOV should be reported, when relevant to patient care.

Reconstruction artifacts. Image artifacts may occur if extracardiac activity is present adjacent to the myocardium. For example, intense focal activity in the liver or the gastrointestinal tract may lead to spillover of residual activity from imperfect scatter compensation resulting in artificially elevated counts or cause a reconstruction (i.e., ramp-filter) artifact resulting in artifactually low count rates in adjacent myocardium. A method to correct for such artifacts is currently not available, but such artifacts, particularly the ramp-filter artifact, are less prominent when iterative reconstruction is used instead of the standard FBP techniques. Additional artifacts can result from problems with CT transmission images, such as streaks caused by insufficient x-ray tube intensity in obese individuals, truncations, beam hardening resulting from bone (e.g., arms down) or metal adjacent to the heart (e.g., pacemakers and internal defibrillators), and breathing leading to disconnected pieces of liver in the lungs or misalignment between CT and PET data. CT artifacts are propagated into the PET images through use of the CT image for attenuation and scatter corrections. These artifacts are less of a problem with Cs-137 attenuation correction.

Image count statistics. The final count density of PET images is influenced by additional factors such as body habitus and weight, radionuclide dose, scanner performance, acquisition time, and in the case of metabolic imaging, the dietary and hormonal state. Image count density directly affects the diagnostic quality and reliability of the study.

Image Analysis and Interpretation of PET Images

The rest and stress perfusion and/or metabolism images, should be interpreted initially without clinical information in order to minimize any bias in study interpretation. All relevant clinical data should be reviewed after a preliminary impression is formed.

LV and RV size. The reader should note whether there is an enlargement of the right ventricle (RV) or LV

at rest or whether there is transient stress-induced LV cavity dilation. Ventricular enlargement seen on the stress and rest perfusion or metabolic images generally indicates left, right, or bi-ventricular dysfunction. Transient stress-induced LV dilation usually reflects extensive CAD. LV and RV sizes as well as any changes associated with stress are typically described qualitatively. A number of commercially developed software packages originally developed for SPECT have the ability to quantify mean LV volumes and end-diastolic and end-systolic volumes for gated PET images, but not all such packages have been validated for all PET instruments, and they should be used with caution.

Lung uptake. Increased tracer activity in the lungs should be reported qualitatively. Increased lung uptake on the perfusion images, particularly when severe, may reflect severe LV dysfunction with increased LV end-diastolic and capillary wedge pressures. It can also reflect infiltrative diseases of the lungs, and can be seen in smokers.

RV uptake. Increased RV tracer uptake may be seen both on perfusion and metabolism images in the presence of pulmonary hypertension with or without significant RV hypertrophy. Assessment of increased RV uptake is usually assessed relative to the radiotracer uptake in the LV myocardium. Since the septum is shared by both ventricles, assessment of increased RV uptake should be made in relation to other regions of the LV myocardium. Abnormally increased RV tracer uptake is a qualitative assessment.

Blood pool activity. Visualization of persistent blood pool activity on either perfusion or metabolism images is usually a sign of relatively poor myocardial uptake of the radiotracer, insufficient time for uptake of the radiotracer into the myocardium, or diminished clearance of the radiotracer from blood. A major cause of increased blood pool activity, especially for perfusion imaging with Rb-82, is impairment of cardiac systolic function that prolongs the circulation time. This is especially relevant when only static images are acquired, because vasodilators typically increase cardiac output and shorten the circulation time. Increased blood pool activity may be seen if the acquisition of images begins prior to 70-170 seconds after Rb-82 administration, especially in patients with a history of congestive heart failure and poor LV function. If Rb-82 perfusion images are acquired serially, an appropriate starting point, after blood pool activity has cleared sufficiently, can be chosen after the acquisition for summing the myocardial tracer uptake images. Judicious adjustment of display threshold and contrast settings can help offset this problem. List mode acquisition allows for the re-processing of images with varying delay times and may be useful for optimizing the quality of reconstructed images.

Extra-cardiac findings. The tomographic images should be carefully examined for uptake of the radiotracer in organs other than the myocardium, particularly in the lungs and the mediastinum. Extra-cardiac uptake of a flow tracer may be of clinical significance, as it may be associated with malignancy and/or an inflammatory process. The 3D maximum intensity projection display, a method of displaying acquired PET images as a rotating 3D display, can be particularly helpful in this regard. When using PET/CT systems, review of the low-resolution CT-based transmission scans can be useful to delineate potentially important ancillary findings, such as pleural and pericardial effusion, coronary and/or aortic calcification, breast, mediastinal or lung mass, and others.

Interpretation of PET Perfusion Data

Perfusion defect location. Myocardial perfusion defects should be identified through careful visual analysis of the reoriented myocardial slices. Perfusion defects should be characterized by extent, severity and location relative to the specific myocardial territory, such as the anterior, lateral, inferior, septal, and/or apical walls. Standardized nomenclature should be used, according to previously published guidelines.[51] RV defects due to scarring and ischemia should be noted.

Perfusion defect severity and extent: Qualitative. Defect extent should be qualitatively estimated by describing the location of the abnormal segments involved (e.g., anterior, inferior, or lateral) as well as the extent in the LV (e.g., ''mid-to-distal'' or ''extending from base to the apex''). The extent of the defect may also be qualitatively described as small (5-10% of the LV), medium (10-20% of the LV), or large (>20% of the LV). A defect of more than 10% of the LV is associated with a higher risk of events. Defect severity is typically expressed qualitatively as mild, moderate, or severe. Severe defects may be considered as those having a tracer concentration equal or similar to background activity, and moderate defects are considered definitely abnormal but visually discernable activity above the background. Mild defects are those with a subtle but definite reduction in regional myocardial tracer.

Stress and rest myocardial perfusion image sets are compared in order to determine the presence, extent, and severity of stress-induced perfusion defects and to determine whether such defects represent regions of myocardial ischemia or infarction. Regions with stress-induced perfusion abnormalities, which have normal perfusion at rest, are termed reversible perfusion defects and represent ischemia. Perfusion abnormalities on stress, which remain unchanged on rest images, are

termed irreversible or fixed defects, and most often represent areas of prior myocardial infarction. When both ischemia and scar are present, the defect reversibility is incomplete, giving the appearance of partial reversibility.

Perfusion defect severity and extent: Semiquantitative scoring system. In addition to the qualitative assessment of perfusion defects, a semiquantitative approach based on a validated segmental scoring system has been developed Table 12). This approach standardizes the visual interpretation of scans, reduces the likelihood of overlooking clinically significant defects, and provides a semiquantitative index that is applicable to diagnostic and prognostic assessments.

A 17-segment model for semiquantitative visual analysis is usually employed.[51] The model is based on three short-axis slices (apical, mid, and basal) to represent most of the LV and one vertical long-axis slice to better represent the LV apex. The basal and mid short-axis slices are divided into six segments. The apical short-axis slice is divided into four segments. A single apical segment is taken from the vertical long-axis slice. Each segment has a specific name (Figure 1). The extent of stress and rest perfusion abnormalities, as well as an estimate of the extent of scarring and ischemia, can be performed by counting the number of segments. Myocardial segments may be assigned to coronary artery territories. Caution should be exercised because the coronary anatomy varies widely among patients. For example, it is not at all uncommon to find segments 9, 10, and 15 of the 17-segment model involved in left anterior descending artery disease. Similarly, segments 5 and 11 of the model may be affected by disease of the right coronary artery.

A well-accepted 5-point scale semi-quantitative visual scoring method is used in direct proportion to the observed count density of the segment, as follows: 0 = no defect, 1 = mildly reduced, 2 = moderately reduced, 3 = severely reduced; 4 = absent activity (Table 12). In addition to individual scores, calculation of summed scores is recommended, in which the summed stress score is the sum of the stress scores of all segments, the summed rest score is the sum of the resting scores of all segments, and the summed difference score is the difference between the summed stress and summed rest scores and serves as a measure of reversibility. The summed scores incorporate the global extent and severity of perfusion abnormality. For example, the summed stress score reflects the extent and severity of perfusion defects at stress and is affected by prior myocardial infarction as well as by stress-induced ischemia. On the other hand, the summed rest score reflects the amount of infarcted and/or hibernating myocardium. The summed difference score is a measure of the extent and severity of stress-induced ischemia.

Before scoring, it is necessary for the interpreting physician to be familiar with the normal regional variation in count distribution of myocardial perfusion PET. No regional variation in tracer uptake has been reported for Rb-82, except for a mild reduction in the apex and base of the LV, consistent with segmentation artifact and/or thinning of the LV myocardium in these locations. Regarding N-13 ammonia, unlike Rb-82 and other SPECT perfusion tracers, the lateral wall uptake may not necessarily be the region with the highest counts, serving as the reference region for normalization. This normal variation should be kept in mind when interpreting lateral perfusion defects with N-13 ammonia PET. Given the variability in the normal distribution of various radiotracers, the patient's polar map may be compared with a reference polar map derived from radiotracer and gender-specific normal database. Ideally, each camera system and acquisition protocol should have its own ''normal'' file but such normal databases are not widely available. The semi-quantitative analysis system provided by a specific vendor should be validated by appropriate studies published in peer-reviewed journals.

Absolute quantification of myocardial blood flow. Quantitative blood flow approaches offer an objective interpretation that is inherently more reproducible than visual analysis. Absolute quantification may aid in assessing the physiologic significance of known coronary artery stenosis, especially when of intermediate severity. Both relative and absolute quantification are particularly useful in describing changes between two studies in the same patient. In addition, quantitative measurements of myocardial blood flow may identify balanced reductions in myocardial blood flow due to multivessel CAD or diffuse, small-vessel disease.

Quantitative assessment of myocardial blood flow in absolute units (e.g., mL/min/gm tissue) has been well established in the literature with N-13 ammonia and O-15 water.[31-35,57-59] It requires the acquisition of images in dynamic mode. The use of list mode acquisition now enables flow quantification in conjunction with perfusion and gated LV and regional function. The added value in terms of diagnosis and prognosis is the subject of active investigation in several centers. ROIs are placed on the LV myocardium and the LV blood pool and are copied to all serially acquired images for generation of myocardial tissue and blood pool time-activity curves. The time-activity curves are corrected for activity spillover from the blood pool to the myocardium and for radioactive decay. They are then fitted with a validated tracer kinetic model, and estimates of myocardial blood flow in milliliters of blood per minute per

grams of myocardium are obtained. Software programs are also available for generating parametric polar maps that display regional myocardial blood flows in absolute units.

Oxygen-15-labeled water is often considered the ideal radiotracer for quantifying myocardial blood flow in absolute terms.[57-59] Because the capillary and sarcolemmal membranes do not exert a barrier effect to the exchange of water, the activity of O-15-labeled water observed in an ROI assigned to the myocardium on the serially acquired images can be described by a one-compartment tracer kinetic model. O-15 water is not FDA approved, and therefore, it is not used clinically in the United States. However, it is used in Europe for clinical imaging.

Quantification of myocardial blood flow with Rb-82 has been more challenging because of its 75 second half-life resulting in noisy myocardial and blood pool time activity curves.[60,61] The kinetic behavior of Rb-82 in tissue can be described by a one- or two-compartment model, that can be fitted using the arterial input function (i.e., obtain from the blood pool concentration of the LV cavity or left atrium) and myocardial time-activity curves at each segment, or even (with sufficient statistics) at each pixel.[60,62-65] The parameters of the model, which include flow, can be estimated using non-linear regression or other techniques. The large number of free parameters and the high noise levels frequently encountered in Rb-82 images mean that simultaneous estimation of all parameters cannot always be performed reliably.[66] The variability of flow estimates can be reduced by fixing certain parameters to physiologically realistic values, but the fact that the extraction fraction of Rb-82 is flow dependent remains a challenge for accurate quantification. Semi-quantitative indices of flow, such as dividing the mean tissue uptake over a certain period by the integral of the blood concentration, may prove more practical for routine use. Many of the error sources approximately cancel out when flow reserve is calculated and first-order corrections can be applied for the variable extraction fraction of Rb-82.[67]

Gated PET images. The ability to acquire cardiac PET images in conjunction with ECG gating is an important development that has not always been available, particularly on 3D scanners. Some systems support ECG gating via list-mode acquisition. In such a mode the positions of all coincidence pairs are recorded along with timing information and input from an ECG machine. These data can be retrospectively processed to produce ECG gated images, ungated images, and if necessary, dynamic images, which represent the activity distribution as a function of time. The flexibility of this mode of acquisition is particularly convenient for quantitative analysis.

ECG gating of the rest and peak stress myocardial perfusion images can provide additional information regarding changes in LV function and volumes that may be useful in identifying 3-vessel CAD with or without left main disease, which may be underestimated on the review of the perfusion images.[68] Unlike ECG gating of the post-stress SPECT images, PET acquisitions take place during peak pharmacologic vasodilation, especially when using ultra short-lived tracers like Rb-82 (acquisitions are shorter than those for N-13 ammonia and, thus, more likely to occur while the patient is at peak pharmacological stress).[69,70] ECG gating of FDG PET images can also provide additional information regarding regional and global LV function and volumes.

Assessment of Myocardial Viability

Detection of viable myocardium plays a central role in the management of patients with LV dysfunction due to CAD. It is based on the recognition that resting LV dysfunction may be reversible, attributable to myocardial hibernation/stunning, and not necessarily due to myocardial scar. As a consequence, its presence signifies a different prognosis and mandates a different treatment paradigm compared with the presence of predominantly non-viable or irreversible damaged tissue. Indeed, the importance of differentiating viable from non-viable tissue is highlighted by the plethora of techniques currently available to perform this task. Myocardial metabolism imaging with PET and FDG uses the preservation of myocardial glucose metabolism, particularly in the presence of resting hypoperfusion as a scintigraphic marker of viable myocardium. It is accomplished with FDG as a tracer of exogenous glucose utilization. The regional myocardial concentrations of this tracer are compared with the regional distribution of myocardial perfusion. Regional increases in FDG uptake relative to regional myocardial blood flow (i.e., perfusion-metabolism mismatch) signify myocardial viability. In contrast, a regional reduction in FDG uptake in proportion to regional reductions in myocardial perfusion (i.e., perfusion-metabolism match) signifies myocardial scar or nonviable tissue. Areas with maintained perfusion, but diminished FDG uptake, also likely reflect regions of jeopardized but viable myocardium since the perfusion tracers reflect active metabolic trapping.

Comparison of myocardial metabolism to perfusion. The comparison of perfusion and metabolism images obtained with PET is relatively straightforward because both image sets are attenuation-corrected. Thus, a relative increase in myocardial metabolism in regions of reduced perfusion by one grade or more, reflect the presence of perfusion-metabolism

mismatch, hence myocardial viability. In contrast, relative decrease in myocardial metabolism that is in proportion to reductions in regional perfusion reflects the presence of perfusion-metabolism match, hence myocardial scar or nonviable tissue.

Special considerations for combining SPECT perfusion with PET metabolism images. In current clinical practice, FDG PET images are often read in combination with SPECT myocardial perfusion images. The interpreting physician should be careful when comparing the non-attenuation-corrected SPECT images with attenuation-corrected FDG PET images. Myocardial regions showing an excessive reduction in tracer concentration as a result of attenuation artifacts, such as the inferior wall in men or the anterior wall in female subjects, may be interpreted as perfusion-metabolism mismatches, resulting in falsely positive perfusion-metabolism mismatches. Two approaches have proved useful for overcoming this limitation:

1. Because assessment of viability is relevant only in myocardium with regional contractile dysfunction, gated SPECT or PET images offer means for determining whether apparent perfusion defects are associated with abnormal regional wall motion.
2. Quantitative analysis with polar map displays that are compared with tracer- and gender-specific databases (for SPECT images) may be a useful aid to the visual interpretation. SPECT perfusion images with attenuation correction are helpful as well.[71,72] However, neither approach is infallible.

For myocardial FDG images acquired with ultra high-energy collimators or with SPECT-like coincidence detection systems, additional problems may be encountered, especially when the images are not corrected for photon attenuation.[73-75] Myocardial regions with severely reduced tracer activity concentrations due to attenuation artifacts on both perfusion and metabolism imaging, such as the inferior wall in men or the anterior wall in women, may be interpreted erroneously as perfusion-metabolism matches. Attenuation of the high-energy 511-keV photons is less than that for the 140-keV photons of Tc-99m or the 60- to 80-keV photons of Tl-201 so that attenuation artifacts are less prominent for FDG images and may result in an apparent mismatch. Furthermore, the lower spatial resolution of SPECT imaging systems for FDG imaging, especially when using high-energy photon collimation and then comparing with Tc-99m or Tl-201 images, causes apparent mismatches for small defects, at the base of the LV, or at the edges or borders of large perfusion defects. Such artifacts resulting from the use of different photon energies can be avoided by using dedicated PET systems for both perfusion and metabolism imaging. Again, use of ECG-gated imaging to demonstrate normal wall motion, quantitative analysis through polar map displays with comparison to radiotracer- and gender-specific databases of normal may aid in the visual interpretation.

Absolute myocardial glucose utilization. Quantitative estimates of myocardial glucose utilization in absolute units of micromoles of glucose per minute per grams of myocardium have not been found to aid in the assessment or characterization of myocardial viability due to the variability in substrate utilization by the myocardium, even when FDG images are acquired during a hyperinsulinemic-euglycemic clamp.[46,47,76] Methods for deriving quantitative estimates of myocardial metabolism require acquisition of serial images for 60 minutes that begin with tracer injection.[42,43] ROIs are placed on the myocardium and the LV blood pool and are copied to all serially acquired images in order to generate myocardial tissue and blood pool time-activity curves. The time-activity curves are corrected for spillover of activity from the blood pool into the myocardium and for radioactive decay. The time-activity curves are then fitted with a validated tracer kinetic model, and estimates of regional myocardial glucose utilization are obtained in micromoles of glucose per minute per grams of myocardium. Measurements of glucose metabolic rates further require determination of glucose concentrations in arterial or arterialized venous blood. Similar to myocardial perfusion, parametric images and polar maps are also available for display of rates of regional myocardial glucose utilization. Regional metabolic rates on such parametric images are coded by a color scale and can be determined noninvasively for any myocardial region through ROIs assigned to the polar map.[77]

Integration of perfusion and metabolism results. The combined evaluation of regional myocardial perfusion and FDG metabolism images allows identification of specific flow-metabolism patterns that are useful to differentiate viable from nonviable myocardium. It is useful to start with a functional assessment, ideally from gated PET or SPECT imaging, as dysfunctional segments are those suitable for evaluation of myocardial viability. If stress perfusion images as well as resting perfusion images are available, jeopardized myocardium can be distinguished from normal myocardium, and myocardium perfused normally at rest but dysfunctional as a result of repetitive stunning can be distinguished from myopathic or remodeled myocardium.

Differences in blood pool concentration of tracers can impact on the apparent match or mismatch of perfusion-FDG images. The separate adjustment of

threshold and contrast settings can help compensate for these discrepancies.

Four distinct resting perfusion-metabolism patterns may be observed in dysfunctional myocardium:[78-83]

1. Normal blood flow associated with normal FDG uptake.
2. Reduced blood flow associated with preserved or enhanced FDG uptake (perfusion-metabolism mismatch).
3. Normal or near-normal blood flow with reduced FDG uptake (reversed perfusion-metabolism mismatch).
4. Proportionally reduced blood flow and FDG uptake (perfusion-metabolism match).

The patterns 1-3 are all indicative of viable myocardium whereas pattern 4 represents nonviable tissue.

Some laboratories have added a fifth pattern, a mild perfusion-metabolism match in which the regional uptake of both the tracer of blood flow and of FDG is mildly to moderately reduced.[80,81,84] Because contractile function in such ''mild'' matches generally does not improve after revascularization, the pattern is subsequently included in the general category of perfusion-metabolism matches. If stress and rest perfusion imaging information is available, it is useful to add an estimate of the extent of stress-inducible ischemia in regions of normal resting perfusion and FDG uptake, in regions with matched resting perfusion-FDG defects, or in regions with resting perfusion FDG-metabolic mismatch. The simultaneous display of stress and rest perfusion and FDG metabolic images is most helpful but not available on all display workstations. In circumstances where only resting perfusion imaging is performed alongside FDG metabolic imaging, besides reporting on the extent of scar and extent of hibernating myocardium, it is useful to indicate that in the absence of corresponding stress myocardial perfusion images, one cannot rule out stress-induced myocardial ischemia.

In circumstances where only stress perfusion imaging is available in combination with FDG metabolic imaging, the following patterns can be found in segments with contractile dysfunction:

1. Stress perfusion defect with preserved FDG uptake indicates ischemic but viable myocardium. Revascularization is generally appropriate since myocardial ischemia is a very strong predictor for recovery of perfusion and function after a successful revascularization. With stress perfusion and FDG metabolic paired images, it is not possible to differentiate between myocardial ischemia, stunning, and hibernation.
2. Stress perfusion defects associated with proportionately decreased or lack of FDG uptake indicate scarred or nonviable myocardium, and revascularization is not recommended.

Qualitative or semiquantitative approaches can be applied to the interpretation of perfusion-metabolism patterns. When comparing FDG metabolism with perfusion images, it is important to first identify the normal reference region (the region with the highest tracer uptake), preferably on the stress myocardial perfusion images. The extent of mismatch or match defect may be small (5-10% of the LV), moderate (10-20% of the LV), or large (>20% of the LV). The severity of a match defect can be expressed as mild, moderate, or severe in order to differentiate between nontransmural and transmural myocardial infarction.

Interpretation of FDG images when perfusion images have not been obtained. Interpretation of FDG images without perfusion images and/or angiographic information and/or without information on regional wall motion is discouraged. The presence of relatively well-preserved FDG uptake in dysfunctional myocardium does not differentiate ischemic from non-ischemic cardiomyopathy. The degree of FDG accumulation over and above regional perfusion helps to assess the relative amount of scar and metabolically viable myocardium. The latter information may significantly influence the power of the test for predicting functional recovery. Therefore, it is recommended that FDG metabolic images be analyzed in conjunction with perfusion images, obtained either with SPECT or, preferably, with PET.

REPORTING OF MYOCARDIAL PERFUSION AND METABOLISM PET STUDIES

Patient Information

The report should start with the date of the study, patient's age, sex, height, and weight or body surface area, as well as the patient's medical identification number.

Indication for Study

Understanding the reason(s) why the study was requested, aids in focusing the study interpretation on the clinical question asked by the referring clinician. In addition, a clear statement for the indication of the study has become an important component of billing for services rendered.

History and Key Clinical Findings

A brief description of the patient's clinical history and findings can contribute to a more appropriate and

comprehensive interpretation of the rest (and stress) perfusion and of the metabolism images. This information may include past myocardial infarctions and their location, revascularization procedures, the patient's angina-related and congestive heart failure-related symptoms, presence of diabetes or hypertension, and other coronary risk factors. Information on regional and global LV function can similarly be important for the interpretation of regional perfusion and metabolism patterns.

A description of the ECG findings may serve as an aid in the study interpretation, such as the presence of Q waves and their location or conduction abnormalities (e.g., LBBB) for exploring septal perfusion and/or metabolic abnormalities.

Type of Study

The imaging protocols should be stated concisely. This should include the type of camera utilized for imaging myocardial perfusion and/or metabolism, for example, PET or PET/CT system, or SPECT perfusion and FDG PET metabolism. For stress myocardial perfusion PET studies, the type of stressor should be clearly indicated, such as treadmill, dipyridamole, adenosine, A2A adenosine receptor agonist, or dobutamine. Radiopharmaceuticals and their radioactivity doses used for the perfusion and the metabolism PET imaging studies should be identified. The acquisition modes and image sequences should be described, such as static or dynamic image acquisition, for stress and rest perfusion imaging, perfusion and metabolism imaging on different days, and the use of gating.

The main body of the report following this introductory descriptive information should then be tailored to the specific clinical question asked by the referring clinician and the procedural approach chosen for answering this question. For example, the report for a stress-rest myocardial PET perfusion study will be different from a report describing and interpreting a myocardial perfusion and myocardial metabolism study. Similarly, the report for a study that includes a stress and rest myocardial perfusion study along with a myocardial metabolism study should be different.

Summary of Stress Data

If myocardial perfusion has been evaluated during stress, the type of the stressor, the stress agent, the dose, route of administration, and time of infusion should be specified. Side effects and symptoms experienced during stress should be reported. If pharmacologic stress was discontinued prematurely, the reasons should be provided.

Hemodynamic and ECG responses during the stress study, including changes in heart rate, blood pressure, development of arrhythmias, conduction abnormalities, and ST-T wave changes and their location should be detailed. Symptoms such as chest pain, shortness of breath, and others during the administration of the stressor and in the recovery phase should be documented.

Summary of Clinical Laboratory Data and Dietary State

Information about the dietary state (e.g., fasting or post-prandial) and about interventions for manipulating plasma glucose levels through, for example, oral or IV administration of glucose or use of the euglycemic hyperinsulinemic clamp, should be given. If pharmacologic measures, such as nicotinic acid derivatives, have been used, this should be described. Furthermore, BG levels, if obtained at baseline or after intervention, should be listed, as they are useful for the interpretation of the metabolic images. If there is an expected abnormal response to a glucose load, this should also be reported.

Image Description and Interpretation: Perfusion

A statement regarding image quality is important. Reduced quality may affect the accuracy of the interpretation. If the cause of the reduced quality is known or suspected, then it should be stated accordingly. This information may prove useful when repeat images are obtained in the same patient.

The report should first describe the relative distribution of the perfusion tracer on the stress images and provide details on regions with decreased radiotracer uptake in terms of the location, extent, and severity of defects. The authors should then describe whether regional myocardial defects seen on stress images become reversible or persist on the corresponding paired rest images. Other findings, such as LV cavity dilatation at rest, transient (stress-induced) LV cavity dilation, lung uptake, concentric LV hypertrophy, asymmetric septal hypertrophy, pericardial photopenia, prominent RV cavity size and hypertrophy, and extra-cardiac abnormalities, should be included in the report. Regional and global LV function should be described from gated PET perfusion and/or metabolism images. The scintigraphic pattern on the stress/rest myocardial perfusion images should then be reported in clinical terms as:

1. Normal.
2. Ischemic.

3. Scarred with/without a history of prior myocardial infarction.
4. An admixture of scarred and ischemic but viable myocardium.
5. Non-ischemic cardiomyopathy.

Quantitative assessment of absolute regional myocardial blood flow is limited to only a few centers with extensive local expertise. Thus, reporting of myocardial blood flow in absolute terms should be made with caution, since FDA approved software for general clinical use is not available at the present time.

Image Description and Interpretation: Metabolism

The report should describe the relative distribution of myocardial perfusion at rest, and the location, extent, and severity of regional perfusion defects. The report should continue with a description of the FDG uptake in the myocardium and indicate the tracer activity concentrations in normally perfused and in hypoperfused myocardium. The adequacy of achieving a glucose-loaded state, as evident from the radiotracer uptake in normally perfused myocardium and also from blood pool activity, should then be reported and be related to the presence of insulin resistance, including impaired glucose tolerance and Type 2 diabetes. This should be related to the residual blood pool activity as additional evidence for inadequate clearance of FDG from blood into tissue and provide the information for low tracer uptake in normally perfused myocardium. Segments with regional dysfunction that exhibit patterns of viable myocardium (i.e., preserved perfusion or decreased perfusion with either preserved or increased FDG uptake) should be identified. Similar reporting should be performed for segments exhibiting a flow-metabolism matched pattern, that is, decreased regional FDG uptake in proportion to decreased regional myocardial perfusion. The presence of viable and non-viable tissue should be reported as a continuum (e.g., predominantly viable or admixture of viable and non-viable tissue).

Findings on semiquantitative or quantitative image analysis approaches may be added. Location and, in particular, extent of viable and non-viable tissue, expressed as a percentage of the LV, is important because it provides important prognostic information on future cardiac events and predictive information on potential outcomes in regional and global LV function, congestive heart failure-related symptoms, and long-term survival after revascularization. Finally, the description of the perfusion-metabolism findings may include a correlation to regional wall motion abnormalities and should indicate the potential for a post-revascularization improvement in the regional and global LV function. The potential for outcome benefit may also be reported.

Final Interpretation

Results should be succinctly summarized and first address whether the study is normal or abnormal. On rare occasions where a definitive conclusion cannot be made, the interpreter should aid the referring clinician by suggesting other tests that may provide further insight into the clinical dilemma. The report should always take into consideration the clinical question that is being asked: is the study requested for CAD detection or myocardial viability assessment? Any potential confounding artifacts or other quality concerns that significantly impact the clinical interpretation of the PET study should be mentioned.

A statement on the extent and severity of perfusion defects, reversibility and mismatch in relation to FDG metabolism, and their implication regarding ischemia, scar, or hibernating myocardium should be made. It may be useful to conclude the report with a summary of the extent and location of myocardial ischemia in relation to vascular territories, as well as the presence and extent of perfusion-metabolism mismatch in patients with chronic ischemic LV dysfunction. LV cavity size, function, and regional wall motion should be reported at rest and during stress with special note of transient ischemic cavity dilatation, if present. A statement as to the implication of the findings should be made.

Comparison should be made to prior studies, and interim changes regarding the presence and extent of myocardial ischemia, scar, or hibernation should be highlighted. On the basis of the scintigraphic findings (e.g., extent of perfusion-metabolism mismatch), the likelihood of recovery of function after revascularization can be estimated. The potential for a post-revascularization improvement in contractile function is low for perfusion-metabolism matched defects, even if the regional reductions in perfusion and in FDG uptake are only mild or moderate. Conversely, the potential for improvements in regional contractile dysfunction is high if perfusion is normal, if both perfusion and FDG uptake are normal, or if FDG uptake is significantly greater than regional perfusion (i.e., mismatch). Finally, the potential of a post-revascularization improvement in the LVEF by at least 5 or more EF units is high if the mismatch affects 20% or more of the LV myocardium.[83,85] Although lesser amounts of mismatch (5-20% of the LV myocardium) may also have potential outcome benefit, with or without improvement in the LVEF.[86,87] The latter may be included in the report at the reporting physician's discretion.

If additional diagnostic clarification seems needed, the physician may recommend an alternative modality. If a CT transmission scan was performed for attenuation correction, clinically relevant CT findings must be reported.

Acknowledgments

Dominique Delbeke, MD, PhD is a consultant for GE Healthcare and Spectrum Dynamics. Stephen L. Bacharach, PhD receives grant support from Siemens Medical Solutions and Philips Healthcare.

Publication and distribution of this document are made possible by corporate support from Bracco Diagnostics Inc.

APPENDIX 1. SAMPLE IV PROTOCOL: PROTOCOL A

A sample protocol for IV glucose loading is presented. This protocol is based on one in use at Vanderbilt University Medical Center, Nashville, TN, and is adapted from Martin et al[48]

1. IV glucose/insulin loading for nondiabetic patients with a BG level <110 mg/dL (<6.11 mmol/L) under fasting condition.
   a. Prepare dextrose/insulin solution: 15 U of regular insulin in 500 mL of 20% dextrose in a glass bottle. The initial 50 mL is discarded through the plastic IV tubing (no filter) to decrease adsorption of the insulin to the tubing.
   b. Prime the patient with 5 U of regular insulin and 50 mL of 20% dextrose (10 g) IV bolus.
   c. Infuse dextrose/insulin solution at a rate of 3 mL · kg^{-1} · h^{-1} for 60 minutes (corresponding to an insulin infusion of 1.5 mU · kg^{-1} · min^{-1} and a glucose infusion of 10 mg · kg^{-1} · min^{-1}). Monitor BG every 10 minutes (goal BG, 100-200 mg/dL [5.56-11.11 mmol/L]).
   d. If BG at 20 min is 100-200 mg/dL (5.56-11.11 mmol/L), preferably <150 mg/dL (8.33 mmol/L), administer FDG intravenously.
   e. If BG is >200 mg/dL (>11.11 mmol/L), administer small IV boluses of 4-8 U of regular insulin until BG decreases to <200 mg/dL (<11.11 mmol/L). Administer FDG intravenously.
   f. Stop dextrose/insulin infusion at 60 minutes and start 20% dextrose at 2-3 mL · kg^{-1} · h^{-1}.
   g. During image acquisition, continue infusion of 20% dextrose at 2-3 mL · kg^{-1} · h^{-1}.
   h. At completion of the acquisition of the images, discontinue infusion, give a snack to the patient, and advise him or her regarding the risk of late hypoglycemia.
   i. ALERT: (1) If BG is >400 mg/dL (>22.22 mmol/L), call the supervising physician immediately. (2) If BG is <55 mg/dL (<3.06 mmol/L) or if the patient develops symptoms of hypoglycemia with BG < 75 mg/dL (<4.17 mmol/L), discontinue dextrose/insulin infusion, administer one amp of 50% dextrose intravenously, and call the supervising physician.
2. IV glucose/insulin loading for diabetic patients or fasting BG is >110 mg/dL (>6.11 mmol/L):
   a. Prepare insulin solution: 100 U of regular insulin in 500 mL of normal saline solution in a glass bottle. The initial 50 mL is discarded through the plastic IV tubing (no filter) to decrease adsorption of the insulin to the tubing.
   b. Prime patient with regular insulin: If fasting BG is >140 mg/dL (>7.76 mmol/L), prime the patient with 10 U of regular insulin IV bolus. If fasting BG is <140 mg/dL (<7.76 mmol/L), prime the patient with 6 U of regular insulin IV bolus.
   c. Infuse insulin solution at a rate of 1.2 mL · kg^{-1} · h^{-1} for 60 minutes (corresponding to an insulin infusion of 4 mU · kg^{-1} · min^{-1}) or for the entire study (to calculate the regional glucose utilization rate).
   d. After 8-10 minutes or when BG is <140 mg/dL (<7.76 mmol/L), start 20% dextrose infusion at 1.8 mL · kg^{-1} · h^{-1} (corresponding to a dextrose infusion of 6 mg · kg^{-1} · min^{-1}).
   e. Monitor BG every 5-10 minutes and adjust dextrose infusion rate to maintain BG at 80-140 mg/dL (4.44-7.76 mmol/L).
   f. After 20-30 minutes of stable BG, administer FDG.
   g. Maintain the IV infusion of insulin plus 20% dextrose for 30-40 minutes after FDG injection or until the end of the scan (to calculate rMGU [rate of glucose utilization]). Some centers confirm FDG uptake particularly in patients with diabetes before discontinuing the clamp.
   h. At completion of the acquisition of the images, discontinue infusion, give a snack to the patient, and advise him or her regarding the risk of late hypoglycemia.
3. For lean patients with type 1 juvenile-onset diabetes mellitus, apply the following protocol:
   1. If fasting BG is <140 mg/dL (<7.76 mmol/L), inject 4 U of regular insulin and infuse insulin solution at 0.3 mL · kg^{-1} · h^{-1} (1 mU · kg^{-1} ·min^{-1}).
   2. After 8-10 minutes of infusion or when BG is <140 mg/dL (<7.76 mmol/L), start 20% dextrose at 2.4 mL · kg^{-1} · h^{-1} (8 mg · kg^{-1} · min^{-1}).

4. Some centers (Munich, Ottawa, and others) have also applied a front-loaded infusion.

    1. About 6 hours after a light breakfast and their usual dose of insulin or oral hypoglycemic, all diabetic patients have a catheter inserted in one arm for glucose and insulin infusion, as well as a catheter in the opposite arm for BG measurement.
    2. At time 0, the insulin infusion is started. Regular insulin is given at 4 times the final constant rate[88] for 4 minutes, then at 2 times the final constant rate for 3 minutes, then at a constant rate for the remainder of the study.
    3. If the BG is >200 mg/dL (>11.11 mmol/L), an additional bolus of insulin is given. An exogenous 20% glucose infusion is started at an initial rate of 0.25 mg $\cdot$ kg^{-1} $\cdot$ min^{-1} and adjusted until steady state is achieved. The BG concentrations are measured every 5 minutes during the insulin clamp. The glucose infusion is adjusted according to the plasma glucose over the preceding 5 minutes.

APPENDIX 2. SAMPLE IV PROTOCOL: PROTOCOL B

A sample protocol for IV glucose loading is presented. Protocol B is based on the protocol in use at the Emory University-Crawford Long Memorial Hospital (Atlanta, GA).[89] This protocol has been used in over 600 subjects (over one-third of whom were diabetic), resulting in good-quality images in over 98% of studies.

1. If fasting BG is <125 mg/dL (<6.94 mmol/L), give 50% dextrose in water (D-50-W), 25 g, intravenously. Hydrocortisone, 20 mg, should be added to the D-50-W to minimize the rather severe pain that can occur at the injection site with D-50-W. This is compatible and avoids the pain that limits patient cooperation. There is no negative effect on the quality of the FDG studies.
2. If fasting BG is between 125-225 mg/dL (6.94-12.5 mmol/L), give D-50-W, 13 g, intravenously.
3. If fasting BG is >225 mg/dL (>12.5 mmol/L), administer regular aqueous insulin as per the following formula: Regular aqueous insulin (dose units) = (BG − 50)/25.
4. After 30-60 minutes, if BG is less than 150 mg/dL (8.33 mmol/L), give FDG intravenously, but if BG is >150 mg/dL (>8.33 mmol/L), give more regular insulin, until BG is <150 mg/dL (<8.33 mmol/L), before giving FDG. Giving FDG when BG is 150-200 mg/dL (8.33-11.11 mmol/L) resulted in many poor-quality studies.

References

1. Zanzonico P. Positron emission tomography: A review of basic principles, scanner design and performance, and current systems. Semin Nucl Med 2004;34:87-111.
2. Machac J, Bacharach SL, Bateman TM, et al. Imaging guidelines for nuclear cardiology procedures: Positron emission tomography myocardial perfusion and glucose metabolism imaging. J Nucl Cardiol 2006;13:e121-51.
3. National Electrical Manufacturers Association. NEMA standards publication NU 2-1994: Performance measurements of positron emission tomographs. Washington, DC: National Electrical Manufacturers Association; 1994.
4. National Electrical Manufacturers Association. NEMA standards publication NU 2-2001: Performance measurements of positron emission tomographs. Washington, DC: National Electrical Manufacturers Association; 2001.
5. National Electrical Manufacturers Association. NEMA standards publication NU 2–2007: Performance measurements of positron emission tomographs. Rosslyn, VA: National Electrical Manufacturers Association; 2007.
6. deKemp RA, Yoshinaga K, Beanlands RS. Will 3D PET enable routine quantification of myocardial blood flow? J Nucl Cardiol 2007;14:380-97.
7. Ter-Pogossian MM, Ficke DC, Yamamoto M. PET I: A positron emission tomograph utilizing photon time-of-flight information. IEEE Trans Med Imaging 1982;1:179-87.
8. Yamamoto M, Ficke DC, Ter-Pogossian MM. Experimental assessment of the gain achieved by the utilization of time-of-flight information in a positron emission tomograph (Super PETT I). IEEE Trans Med Imaging 1982;1:187-92.
9. Lewellan TK. Time-of-flight PET. Semin Nucl Med 1998;28:268-75.
10. Le Meunier L, Maass-Moreno R, Carrasquillo JA, Dieckmann W, Bacharach SL. PET/CT imaging: Effect of respiratory motion on apparent myocardial uptake. J Nucl Cardiol 2006;13:821-30.
11. International Electrotechnical Commission. Radionuclide imaging devices–characteristics and test conditions. Part 1: Positron emission tomographs. Geneva; 1998.
12. American College of Radiology. ACR Web site. http://www.acr.org. Accessed 2 March 2009.
13. American Association of Physicists in Medicine. AAPM Web site. http://www.aapm.org. Accessed 2 March 2009.
14. Sampson UK, Dorbala S, Limaye A, et al. Diagnostic accuracy of rubidium-82 myocardial perfusion imaging with hybrid positron emission tomography/computed tomography in the detection of coronary artery disease. J Am Coll Cardiol 2007;49:1052-8.
15. Slomka PJ, LeMunier L, Hayes SW. Comparison of myocardial perfusion Rb-82 PET performed with CT- and transmission CT-based attenuation correction. J Nucl Med 2008;49:1992-8.
16. Gould KL, Pan T, Loughin C, Johnson NP, Guha A, Sdringola S. Frequent diagnostic errors in cardiac PET/CT due to misregistration of CT attenuation and emission PET images: A definitive analysis of causes, consequences and corrections. J Nucl Med 2007;48:1112-21.
17. Loghin C, Sdringola S, Gould K. Common artifacts in PET myocardial perfusion images due to attenuation-emission misregistration: Clinical significance, causes, and solution. J Nucl Med 2004;45:1029-39.
18. Alessio AM, Kohlmyer S, Branch K, et al. Cine CT for attenuation correction in cardiac PET/CT. J Nucl Med 2007;48:794-801.
19. Souvatzoglou M, Bengel F, Busch R, et al. Attenuation correction in cardiac PET/CT with three different CT protocols: A

comparison with conventional PET. Eur J Nucl Med Mol Imaging 2007;34:1991-2000.
20. DiFilippo FP, Brunken RC. Do implanted pacemaker leads and ICD leads cause metal-related artifact in cardiac PET/CT? J Nucl Med 2005;46:436-43.
21. Greenland P, Bonow RO, Brundage BH, et al. ACCF/AHA 2007 clinical expert consensus document on coronary artery calcium scoring by computed tomography in global cardiovascular risk assessment and in evaluation of patients with chest pain: A report of the American College of Cardiology Foundation Clinical Expert Consensus Task Force. J Am Coll Cardiol 2007;49:378-402.
22. Hamill JJ, Brunken RC, Bybel B, DiFilippo FP, Faul DD. A knowledge-based method for reducing attenuation artifacts caused by cardiac appliances in myocardial PET/CT. Phys Med Biol 2006;51:2901-18.
23. Henzlova MJ, Cerqueira MD, Hansen CL, Taillefer R, Yao S. Imaging guidelines for nuclear cardiology procedures: Stress protocols and tracers. J Nucl Cardiol 2009;16. doi: 10.1007/s12350-009-9062-4.
24. Beanlands RS, Chow BJW, Dick A, et al. CCS/CAR/CANM/CNCS/CanSCMR joint position statement on advanced noninvasive cardiac imaging using positron emission tomography, magnetic resonance imaging n multi-detector computed tomographic angiography in the diagnosis and evaluation of ischemic heart disease—executive summary. Can J Cardiol 2007;23:107-19.
25. Bateman TM, Friedman JD, Heller GV, et al. Diagnostic accuracy of rest/stress ECG-gated Rb-82 myocardial perfusion PET: Comparison with ECG-gated Tc-99m sestamibi SPECT. J Nucl Cardiol 2006;13:24-33.
26. Love WD, Burch GE. Influence of the rate of coronary plasma on the extraction of rubidium-86 from coronary blood. Circ Res 1959;7:24-30.
27. Selwyn AP, Allan RM, L'Abbate A, et al. Relation between regional myocardial uptake of rubidium-82 and perfusion: Absolute reduction of cation uptake in ischemia. Am J Cardiol 1982;50:112-21.
28. Goldstein RA, Mullani NA, Marani SK, et al. Myocardial perfusion with rubidium-82. II. Effects of metabolic and pharmacologic interventions. J Nucl Med 1983;24:907-15.
29. Stabin MG. Radiopharmaceuticals for nuclear cardiology: Radiation dosimetry, uncertainities and risk. J Nucl Med. 2008;49:1555–63.
30. Camici PG, Araujo LI, Spinks T, et al. Increased uptake of 18F-fluorodeoxyglucose in postischemic myocardium of patients with exercise-induced angina. Circulation 1986;74:81-8.
31. Chow BJW, Ananthasubramaniam K, deKemp RA, et al. Comparison of treadmill exercise versus dipyridamole stress with myocardial perfusion imaging using rubidium-82 positron emission tomography. J Am Coll Cardiol 2005;45:1227-34.
32. Hutchins GD, Schwaiger M, Rosenspire KC, et al. Noninvasive quantification of regional blood flow in the human heart using N-13 ammonia and dynamic positron emission tomographic imaging. J Am Coll Cardiol 1990;15:1032-42.
33. Krivokapich J, Smith GT, Huang SC, et al. 13 N ammonia myocardial imaging at rest and with exercise in normal volunteers. Quantification of absolute myocardial perfusion with dynamic positron emission tomography. Circulation 1989;80:1328-37.
34. Bergmann SR, Hack S, Tewson T, Welch MJ, Sobel BE. The dependence of accumulation of N-13 ammonia by myocardium on metabolic factors and its implications for quantitative assessment of perfusion. Circulation 1980;61:34-43.
35. Krivokapich J, Huang S-C, Phelps ME, MacDonald NS, Shine KI. Dependence of N-13 ammonia myocardial extraction and clearance on flow and metabolism. Am J Physiol: Heart Circ Physiol 1982;242:H536-42.
36. Kitsiou AN, Bacharach SL, Bartlett ML, et al. 13 N ammonia myocardial blood flow and uptake: Relation to functional outcome of asynergic regions after revascularization. J Am Coll Cardiol 1999;33:678-86.
37. Schelbert HR, Phelps ME, Huang SC, et al. N-13 ammonia as an indicator of myocardial blood flow. Circulation 1981;63:1259-72.
38. International Commission on Radiological Protection. Radiation dose to patients from radiopharmaceuticals. ICRP Publication 80. Ann ICRP 2000;28:113.
39. International Commission on Radiological Protection. Radiation dose to patients from radiopharmaceuticals. ICRP Publication 53. Ann ICRP 1988;18:62.
40. Neely JR, Rovetto MJ, Oram JF. Myocardial utilization of carbohydrate and lipids. Prog Cardiovasc Dis 1972;15:289-329.
41. Gallagher BM, Ansari A, Atkins H, et al. Radiopharmaceuticals XXVII. F-18-labeled 2-deoxy-2-fluoro-D-glucose as a radiopharmaceutical for measuring regional myocardial glucose metabolism in vivo: Tissue distribution and imaging studies in animals. J Nucl Med 1977;18:990-6.
42. Ratib O, Phelps ME, Huang SC, et al. Positron tomography with deoxyglucose for estimating local myocardial glucose metabolism. J Nucl Med 1982;23:577-86.
43. Hamacher K, Coenen HH, Stauocklin G. Efficient sterospecific synthesis of no-carrier-added 2-[F-18]-fluoro-2-deoxy-D-glucose using aminopolyether supported nucleophilic substitution. J Nucl Med 1986;27:235-8.
44. CDE Inc. Dosimetry Services. Dose estimates: Adult. http://www.internaldosimetry.com/freedosestimates/adult/index.html. Published 2001. Accessed 15 January 2009.
45. Ohtake T, Yokoyama I, Watanabe T, et al. Myocardial glucose-metabolism in noninsulin-dependent diabetes-mellitus patients evaluated by FDG-PET. J Nucl Med 1995;36:456-63.
46. Vitale GD, deKemp RA, Ruddy TD, Williams K, Beanlands RS. Myocardial glucose utilization and optimization of (18)F-FDG PET imaging in patients with non-insulin-dependent diabetes mellitus, coronary artery disease, and left ventricular dysfunction. J Nucl Med 2001;42:1730-6.
47. Knuuti MJ, Nuutila P, Ruotsalainen U, et al. Euglycemic hyperinsulinemic clamp and oral glucose load in stimulating myocardial glucose utilization during positron emission tomography. J Nucl Med 1992;33:1255-62.
48. Martin WH, Jones RC, Delbeke D, Sandler MP. A simplified intravenous glucose loading protocol for fluorine-18 fluorodeoxyglucose cardiac single-photon emission tomography. Eur J Nucl Med 1997;24:1291-7.
49. Gropler RJ, Siegel BA, Lee KJ, et al. Nonuniformity in myocardial accumulation of fluorine-18-fluorodeoxyglucose in normal fasted humans. J Nucl Med 1990;31:1749-56.
50. Bax JJ, Veening MA, Visser FC, et al. Optimal metabolic conditions during fluorine-18 fluorodeoxyglucose imaging; a comparative study using different protocols. Eur J Nucl Med 1997;24:35-41.
51. Cerqueira MD, Weissman NJ, Dilsizian V, et al. Standardized myocardial segmentation and nomenclature for tomographic imaging of the heart: A statement for healthcare professionals from the Cardiac Imaging Committee of the Council on Clinical Cardiology of the American Heart Association. J Nucl Cardiol 2002;9:240-5.
52. Porenta G, Kuhle W, Czernin J, et al. Semiquantitative assessment of myocardial blood flow and viability using polar map displays of cardiac PET images. J Nucl Med 1992;33:1628-36.

53. Nekolla SG, Miethaner C, Nguyen N, Ziegler SI, Schwaiger M. Reproducibility of polar map generation and assessment of defect severity and extent assessment in myocardial perfusion imaging using positron emission tomography. Eur J Nucl Med 1998;25: 1313-21.
54. Dou K, Yang M, Yang Y, Jain D, He Z. Myocardial 18F-FDG uptake after exercise-induced myocardial ischemia in patients with coronary artery disease. J Nucl Med 2008;49:1986-91.
55. Dilsizian V. SPECT and PET myocardial perfusion imaging: Tracers and techniques. In Dilsizian V, Narula J, editors. Atlas of Nuclear Cardiology, edition 3. Barunwald E (series editor), Philadelphia, Current Medicine, Inc. - Springer; 2009, p. 37-60.
56. McCord ME, Bacharach SL, Bonow RO, et al. Misalignment between PET transmission and emission scans: Its effect on myocardial imaging. J Nucl Med 1992;33:1209-14.
57. Bergmann SR, Fox KAA, Rand AL, et al. Quantification of regional myocardial blood flow in vivo with O-15 water. Circulation 1984;70:724-33.
58. Bergmann SR, Herrero P, Markham J, Weinheimer CJ, Walsh MN. Noninvasive quantitation of myocardial blood flow in human subjects with oxygen-15-labeled water and positron emission tomography. J Am Coll Cardiol 1989;14:639-52.
59. Iida H, Kanno I, Takahashi A, et al. Measurement of absolute myocardial blood flow with O-15 water and dynamic positron emission tomography. Circulation 1988;78:104-15.
60. Lortie M, Beanlands RS, Yoshinaga K, et al. Quantification of myocardial blood flow with 82Rb dynamic PET imaging. Eur J Nucl Med Mol Imaging 2007;34:1765-74.
61. Lin JW, Sciacca RR, Chou RL, Laine AF, Bergmann SR. Quantification of myocardial perfusion in human subjects using 82Rb and wavelet-based noise reduction. J Nucl Med 2001;42:201-8.
62. Herrero P, Markham J, Shelton ME, Weinheimer CJ, Bergmann SR. Noninvasive quantification of regional myocardial perfusion with rubidium-82 and positron emission tomography exploration of a mathematical model. Circulation 1990;82:1377-86.
63. Herrero P, Markham J, Shelton ME, Bergmann SR. Implementation and evaluation of a two-compartment model for quantification of myocardial perfusion with rubidium-82 and positron emission tomography. Circ Res 1992;70:496-507.
64. El Fakhri G, Sitek A, Guerin B, et al. Quantitative dynamic cardiac 82 Rb PET using generalized factor and compartment analyses. J Nucl Med 2005;46:1264–71.
65. El Fakhri G, Sitek A, Abi-Hatem N, et al (2009) Reproducibility and accuracy of quantitative myocardial blood flow: A PET study comparing 82 Rubidium and 13 N-Ammonia. J Nucl Med. in press
66. Coxson PG, Huesman RH, Borland L. Consequences of using a simplified kinetic model for dynamic PET data. J Nucl Med 1997;38:660-7.
67. Yoshida K, Mullani N, Gould KL. Coronary flow and flow reserve by PET simplified for clinical applications using rubidium-82 or nitrogen-13 ammonia. J Nucl Med 1996;37:1701-12.
68. Lertsburapa K, Ahlberg A, Bateman T, et al. Independent and incremental prognostic value of left ventricle ejection fraction determined by stress gated rubidium 82 PET imaging in patients with known or suspected coronary artery disease. J Nucl Cardiol 2008;15:745-53.
69. Dorbala S, Vangala D, Sampson U, et al. Value of vasodilator left ventricular ejection fraction reserve in evaluating the magnitude of myocardium at risk and the extent of angiographic coronary artery disease: A 82Rb PET/CT study. J Nucl Med. 2007;48:349–58.
70. Dorbala S, Hachamovitch R, Curillova Z, et al (2009) Incremental prognostic value of gated Rb-82 positron emission tomography over clinical variables and rest LVEF. J Am Coll Cardiol Img 2009 2:846-854.
71. Heller GV, Links J, Bateman TM, et al. American Society of Nuclear Cardiology and Society of Nuclear Medicine joint position statement: Attenuation correction of myocardial perfusion SPECT scintiography. J Nucl Cardiol 2004;11:229-30.
72. Malkerneker D, Brenner R, Martin WH, et al. CT-based attenuation correction versus prone imaging to decrease equivocal interpretations of rest/stress 99mTc-tetrafosmin SPECT MPI. J Nucl Cardiol 2007;14:314-23.
73. Sandler MP, Videlefsky S, Delbeke D, et al. Evaluation of myocardial ischemia using a rest metabolism/stress perfusion protocol with fluorine-18-fluorodeoxyglucose/technitium-99m-MIBI and dual-isotope simultaneous-acquisition single-photon emission computed tomography. J Am Coll Cardiol 1995;26:870-6.
74. Bax JJ, Visser FC, Blanksma PK, et al. Comparison of myocardial uptake of fluorine-18-fluorodeoxyglucose imaged with PET and SPECT in dyssynergic myocardium. J Nucl Med 1996;37:1631-6.
75. Dilsizian V, Bacharach SL, Muang KM, Smith MF. Fluorine-18-deoxyglucose SPECT and coincidence imaging for myocardial viability: Clinical and technological issues. J Nucl Cardiol 2001;8:75-88.
76. Choi Y, Brunken RC, Hawkins RA, et al. Factors affecting myocardial 2-[F-18] fluoro-2-deoxy-D-glucose uptake in positron emission tomography studies of normal humans. Eur J Nucl Med 1993;20:308-18.
77. Choi Y, Hawkins RA, Huang SC, et al. Parametric images of myocardial metabolic rate of glucose generated from dynamic cardiac PET and 2-[18F]fluoro-2-deoxy-D-glucose studies. J Nucl Med 1991;32:733-8.
78. Marshall RC, Tillisch JH, Phelps ME, et al. Identification and differentiation of resting myocardial ischemia and infarction in man with positron emission tomography, F-18 labeled fluorodeoxyglucose and N-13 ammonia. Circulation 1983;67:766-8.
79. Tillisch J, Brunken RC, Marshall R, et al. Reversibility of cardiac wall-motion abnormalities predicted by positron tomography. N Engl J Med 1986;314:884-8.
80. Schwartz E, Schaper J, vom Dahl J, et al. Myocardial hibernation is not sufficient to prevent morphological disarrangements with ischemic cell alterations and increased fibrosis. Circulation 1994;90:I-378.
81. vom Dahl J, Altehoefer C, Sheehan F, et al. Recovery of regional left ventricular dysfunction after coronary revascularization: Impact of myocardial viability assessed by nuclear imaging and vessel patency at follow-up angiography. J Am Coll Cardiol 1996;28:948-58.
82. Beanlands RS, Hendry PJ, Masters RG, et al. Delay in revascularization is associated with increased mortality rate in patients with severe left ventricular dysfunction and viable myocardium on fluorine 18-fluorodeoxyglucose positron emission tomography imaging. Circulation 1998;98:II51-6.
83. Gerber BL, Ordoubadi FF, Wijns W, et al. Positron emission tomography using (18)F-fluoro-deoxyglucose and euglycaemic hyperinsulinaemic glucose clamp: Optimal criteria for the prediction of recovery of post-ischaemic left ventricular dysfunction. Results from the European Community Concerted Action Multicenter study on the use of (18)F-fluoro-deoxyglucose positron emission tomography for the detection of myocardial viability. Eur Heart J 2001;22:1691-701.
84. Bonow RO, Dilsizian V, Cuocolo A, Bacharach SL. Identification of viable myocardium in patients with coronary artery disease and left ventricular dysfunction: Comparison of thallium scintigraphy with reinjection and PET imaging with 18F-fluorodeoxyglucose. Circulation 1991;83:26-37.
85. Pagano D, Townend JN, Littler WA, et al. Coronary artery bypass surgery as treatment for ischemic heart failure: The predictive

value of viability assessment with quantitative positron emission tomography for symptomatic and functional outcome. J Thorac Cardiovasc Surg 1998;115:791-9.
86. Di Carli MF, Davidson M, Little R, et al. Value of metabolic imaging with positron emission tomography for evaluating prognosis in patients with coronary artery disease and left ventricular dysfunction. Am J Cardiol 1994;73:527-33.
87. Beanlands RS, Nichol G, Huszti E, et al. F-18-fluorodeoxyglucose positron emission tomography imaging-assisted management of patients with severe left ventricular dysfunction and suspected coronary artery disease: A randomized, controlled trial (PARR-2). J Am Coll Cardiol 2007;50:2002-12.
88. DeFronzo RA, Tobin JD, Andres R. Glucose clamping technique: A method for quantifying insulin secretion and resistance. Am J Physiol 1979;237:E214-23.
89. Streeter J, Churchwell K, Sigman S, et al. Clinical glucose loading protocol for F-18 FDG myocardial viability imaging [abstract]. Mol Imaging Biol 2002;4:192.